ISSN 0965-5441, Petroleum Chemistry, 2023, Vol. 63, No. 10, pp. 1143–1169. © Pleiades Publishing, Ltd., 2023.
ISSN 0965-5441, Petroleum Chemistry, 2024. © Pleiades Publishing, Ltd., 2024.
Russian Text © The Author(s), 2023, published in Neftekhimiya, 2023, Vol. 63, No. 6, pp. 775–808.

Hydrotreating of Lignocellulosic Bio-Oil (A Review)

G. O. Zasypalov[a, *], V. A. Klimovsky[a], E. S. Abramov[a], E. E. Brindukova[b], V. D. Stytsenko[a], and A. P. Glotov[a]

[a] *Gubkin Russian State University of Oil and Gas (National Research University), Moscow, 119991 Russia*
[b] *Kursk State Agricultural Academy, Kursk, 305021 Russia*
**e-mail: gleb.zasypalov@mail.ru*

Received September 14, 2023; revised November 27, 2023; accepted December 6, 2023

Abstract—This review discusses recent advances in catalytic hydrodeoxygenation of lignocellulosic biomass. Lignocellulosic biomass is the most promising plant-based raw material for the production of liquid engine fuels or individual petrochemical monomers. Among the several existing techniques for biomass processing, pyrolysis offers superior efficiency. Given that the bio-oil produced by biomass pyrolysis has unsatisfactory performance characteristics caused by the presence of oxygenates, this bio-oil cannot be used directly as a fuel. Hydrodeoxygenation using selective catalysts is able to reduce the oxygen content in bio-oil and to improve its performance characteristics. To this end, bifunctional catalysts that contain active metal sites on an acid support hold promise. Noble metals (e.g., Pt, Pd, and Ru) and/or transition metals (e.g., Ni, Co, and Mo), as well as sulfides and phosphides of transition metals, can be used as an active catalytic phase. Metal oxides (e.g., ZrO_2, CeO_2, Al_2O_3, and TiO_2), carbon, zeolites (e.g., ZSM-5, Y, Beta, and SAPO-11), and mesoporous silica-based materials (e.g., SBA-15 and MCM-41) have been most often used as supports in hydrodeoxygenation catalysts. However, the implementation and upscaling of the hydrodeoxygenation of biomass pyrolytic bio-oil is limited because of the rapid deactivation of the catalyst in the presence of water, due to sintering and leaching the active phase with acidic components of bio-oil. Therefore, the development of catalysts that would provide high activity and stability under bio-oil hydrodeoxygenation conditions has become one of the most pressing issues for the petrochemical industry.

Keywords: hydrodeoxygenation, bio-oil, pyrolysis, zeolites, aluminosilicates, halloysite

DOI: 10.1134/S0965544123090013

In view of the global annual reduction in the consumption of fossil energy resources, the refining and petrochemical industries are facing a pressing scientific and engineering problem that will need to be solved by developing alternative energy. However, the 2019–2022 COVID-19 pandemic has diminished the importance of green energy to some extent. Specifically, the oil market collapse caused by the pandemic, and exacerbated by the OPEC+ failure to come to an agreement on production and pricing, turned crude oil from a valuable energy source into a virtually worthless material [1]. The uncertainty in the fossil fuel market environment and the high dependence on oil and gas imports still leads world investors to count on alternative energies [2]. One promising solution to this challenge of reducing crude oil consumption involves using renewable plant-based raw materials for the production of engine fuels and valuable petrochemical monomers [3]. Particular attention has been paid to non-food lignocellulosic biomass due to its carbon neutrality and widespread availability [4]. Bearing in mind that lignocellulosic biomass is a waste product of the wood processing industry, this material most certainly holds great promise as a substitute for fossil energy [5].

The main components of lignocellulosic biomass are cellulose, hemicellulose, and lignin [6]. Lignin is of particular interest from the viewpoint of downstream processing because its macromolecule mainly consists of aromatic units linked by ether and carbon bonds, thus forming a set of phenylpropane structural units [7]. Depolymerization of these units allows valuable compounds such as phenol, benzene, eugenol, cresol, resorcinol, and vanillin to be produced from lignin. For the depolymerization and defragmentation of this type of renewable raw materials, one promising technique is pyrolysis, an oxygen-free thermal process that produces both gases, liquids (in this case, bio-oil), and solid residues

[8]. Bio-oil is a mixture of compounds, principally low-molecular-weight alcohols, acids, esters, ethers, aldehydes, ketones, furans, and phenols [9]. Along with organic oxygenates, bio-oil contains about 30–50 wt % of water. Although this limits the direct use of bio-oil as a component of engine fuels, the bio-oil quality can be substantially improved using the catalytic hydrotreating (specifically by hydrodeoxygenation, HDO). Moreover, the low nitrogen content (below 0.02 wt %) and complete absence of sulfur in bio-oil make it even more attractive [10]. The HDO improves the physicochemical properties of the refined product via conversion of a major portion of oxygenates to water and carbon dioxide. Most importantly, HDO products can be readily mixed with petroleum feedstocks, thus offering an opportunity for their co-processing [11].

The HDO of the lignocellulosic bio-oil is based upon bifunctional catalysts comprising hydrogenation and acid sites [12]. Therefore, the activity and selectivity of catalysts are largely determined by the structure and acidity of the supports, most often zeolites [13]. However, their high acidity induces cracking of intermediates, thus decreasing the selectivity to final product [14]. Furthermore, the microporous structure of zeolites hinders the diffusion of branched organic substrates towards active sites and, thus, diminishes the conversion of the lignocellulose feedstock.

The challenges mentioned above can be overcome by developing new approaches that will facilitate the invention of innovative mesoporous and micro–mesoporous catalysts comprising various types of structured aluminosilicates. These catalysts should be specifically created for the conversion of lignocellulosic bio-oil to environmentally friendly fuel components and valuable petrochemicals.

The purpose of this study is the summarization and assessment of the existing bio-oil production methods and the major bio-oil processing routes. Moreover, there will be considered peculiarities of HDO implementation using various types of catalytic systems as well as the evaluation of effects of metals, supports, and techniques of their modification on the activity, selectivity, and stability of lignin HDO.

BIOFUEL TYPES: CLASSIFICATION AND CHARACTERIZATION

In recent decades, the world economy has faced two major challenges that directly relate to the power industry: the increasing energy scarcity and climate change [15]. The obvious preventive measure to combat both challenges is partial or complete replacement of fossil fuels with renewable raw materials. The most common biofuels (e.g., biodiesel, bioethanol, biogas, and biohydrogen) are known to be produced from organic biomass and lignocellulosic feedstocks [16]. Depending on the feedstock type, biofuels are commonly classified into three generations.

First-generation biofuels include products derived from food biomass (e.g., sugar and starch derivatives), namely bioethanol (BE) and biodiesel (BD), the world commercial production of which currently amounts to about 50 million tons annually [17]. **Second-generation** biofuels are produced from non-food biomass such as wood, rice husk, flaxseed, or food processing wastes [18, 19]). **Third-generation** biofuels include microalgae-derived products derived from microalgae [20].

The first-generation high-purity BE produced by fermentation of sugar- and starch-based crops [21] can be used in engine fuels by being added to gasoline. A 90:10 (v/v) gasoline–BE blend is known as E10 [22]. Furthermore, BE serves as a raw material to produce ethylbutyl ether, a high-octane oxygenate [23]. However, despite the advances in the production of first-generation BE, a number of constraints still interfere with its commercialization [24]. BE production from food feedstocks raises a major issue: use of lands suitable for bio-energy crop production [25]. An analysis of the food and energy markets has demonstrated that the increasing demand for BE, and the corresponding increase in its food-based production, have contributed to a 10–25% food price increase [26]. Therefore, it is preferable to produce second-generation BE, either biologically (from non-food biomass feedstocks [24]) or synthetically (by conventional catalytic hydration of ethylene [27]).

First-generation BD is produced from animal fats and vegetable oils by transesterification with methanol or ethanol [28]. The average food-derived BD contains hydrocarbons (HCs) produced by exhaustive hydrogenation of C_{12}–C_{18} fatty acid esters. Like BE, BD can be used both in blends with conventional diesel fuels (the blends with BD content of 5, 7, 10, and 20 vol % are known as B5, B7, B10, and B20, respectively) and in the pure form (B100; this case, however, requires the engine and fuel supply designs to be appropriately modified, like in the BE case) [29]. To ensure that pure or blended BD successfully competes with conventional diesel fuels,

Table 1. Physicochemical properties of biodiesel versus petroleum diesel [31]

Physicochemical properties	Petroleum diesel	Biodiesel
Density at 15°C, kg/m^3	838–872	852–922
Kinematic viscosity at 40°C, mm^2/s	2–3	4–4.5
Flash point, °C	50–98	70–241
Cloud point, °C	–17 to –8	–5 to –6
Pour point, °C	–36 to –30	–20 to –15
Cetane number	40–45	45–50
Energy density, MJ/kg	45	34
Average molecular weight, g/mol	170	293
Carbon content, wt %	86.80	76.20
Hydrogen content, wt %	13.20	12.60
Oxygen content, wt %	0.00	11.20
H/C	1.85	1.98
O/C	–	0.11

Table 2. Physicochemical properties of biofuels and conventional fossil fuels [39, 40]

Parameter	Fossil		Plant-based	
	vacuum gasoil	diesel fuel	bio-oil	bio-oil after HDO
Density, kg/m^3	936–937	880	1050–1250	930
Dynamic viscosity at 50°C, cSt	180	2.71	40–100	1–5
pH	–	–	2.8–3.8	5.8
Energy density, MJ/kg	40	38	16–19	42–45
H_2O content, wt %	0.1	–	15–30	1.5
S content, wt %	0.59–0.67	<0.001	<0.05	<0.005
N content, wt %	0.33–0.34	–	<0.4	–
O content, wt %	1	–	28–40	<5
H/C ratio	1.6	1.85	0.9–1.5	1.3–2.0
O/C ratio	<0.01	–	0.3–0.5	<0.1

it must satisfy the specifications of ASTM D6751 (or EN 14214) as the generally recognized standard [30]. Table 1 presents the physicochemical properties of BD versus conventional diesel fuels.

Second-generation biofuels are generally produced by processing non-food raw materials (e.g., wood biomass, food and agricultural wastes, waste fats, vegetable oils, etc.) [32]. Second-generation biofuel production does not compete with the food industry, and the cultivation of these feedstocks requires no arable land, equipment, or fertilizers to be used. Moreover, due to the transformation of an entire plant (rather than its part) into energy, the production of second-generation biofuels from wheat straw, hardwoods, or softwoods has achieved higher yields than that of first-generation biofuels [33].

Pyrolysis, an oxygen-free process carried out at high temperatures, holds promise for processing lignocellulosic biomass into biofuels, including pyrolysis gas, bio-oil, and biochar as a solid residue [34]. The yield of pyrolysis products depends on the feedstock type and process conditions. The most valuable product of the flash pyrolysis of lignocellulosic biomass is bio-oil, the yield of which has reached 60–75 wt % [35]. Plant-based bio-oil is an environmentally friendly raw material for the production of engine fuels essentially free of sulfur and nitrogen compounds [36]. However, bio-oil produced by the pyrolysis of lignocellulosic biomass has a number of critical drawbacks associated with its high (35–40 wt %) oxygen content [37], high viscosity, high acidity, tendency to polymerization, and low heating value (Table 2). Although these drawbacks limit the application range of

Table 3. Physicochemical properties of bio-oil produced by pyrolysis of algal and lignocellulosic biomass [47]

Parameter	Bio-oil derived from lignocellulosic biomass	Bio-oil derived from microalgal biomass
Carbon content, wt %	56.40	62.07
Hydrogen content, wt %	6.20	8.76
Oxygen content, wt %	37.30	11.24
Nitrogen content, wt %	0.10	9.74
Density, kg/dm^3	1.20	1.06
Dynamic viscosity at 40°C, cP	40–200	100
Energy density, MJ/kg	19	27

bio-oil as a component of engine fuels, its quality can be appreciably improved by catalytic hydrotreating such as HDO. Table 2 presents the comparative characteristics of fuels produced from mineral and vegetable raw materials. Importantly, the HDO may be performed with the use of catalysts sensitive to poisons as far as bio-oil is free of sulfur and nitrogen compounds [38].

The cost effectiveness of lignocellulosic biomass processing treatment has been demonstrated for the case of the IH^2 technology offered by CRI Catalyst Company. The production cost of the lignocellulose-derived fuels has been assessed as about \$0.53/L, compared to the prices of conventional gasoline and diesel (\$0.76 and 0.82/L, respectively, net of taxes, logistics costs, and marketing expenditures) [41]. Moreover, the production cost of the distillates obtained by lignocellulose hydrotreatment has been additionally reduced by integrating the production with a manufacturing facility that possesses a well-developed technology infrastructure (e.g., a paper mill or a refinery) [42].

The algae-based production of third-generation biofuels has a number of advantages such as environmental friendliness, high fat content, and the ability of algae to grow both in artificial and natural environments [43]. Adequate light intensity, a fairly small space, and the presence of carbon dioxide and other (inorganic) nutrients are sufficient conditions to cultivate algae [44].

Pyrolysis has been recognized as the most efficient technology for the production of third-generation biofuels. In terms of their properties, the bio-oil produced by pyrolysis of algal biomass is similar to wood-derived bio-oil. The former bio-oil has a high oxygen content and, hence, low heating value, high viscosity, and high acidity [46]. All these properties limit the usability of third-generation bio-oil in combustion engines, so the product should be hydrofinished. In addition, the bio-oil produced by pyrolysis of algal biomass has the high nitrogen content (10 wt %) that must be duly considered given the nitrogen compounds usually are catalytic poisons (Table 3) [38].

The 2022 market for algae-derived products amounted to \$4.9 billion. Their production is forecasted to be about \$5.3 billion by the end of 2023 and to further grow by 6.4% annually, so it may reach \$7.3 billion by 2028. As a nascent technology, algae biorefineries are still not commercially feasible because they cannot be economically viable solely based on the lipid production [20]. Instead, an entire portfolio of value-added algal products will be needed to complement the lipids and make algae profitable. To implement commercial production, large-scale algae farms and infrastructure of algae biorefineries—currently lacking—must be built.

BIO-OIL: PRODUCTION METHODS AND COMMERCIAL TECHNOLOGIES

Currently, three main process approaches are generally applied to biomass conversion: chemical, biochemical, and thermochemical [29].

Chemical conversion of biomass, an approach generally based on transesterification and applicable to the conversion of oilseeds [48] or microalgae [49], is unsuitable for the production of second-generation biofuels.

Biochemical conversion is a highly selective technique that provides the high yeild production of bioethanol, biobutanol, biodiesel, and other biochemicals [50]. However, out of more than sixty processes developed for the biochemical conversion of plant-based raw materials, only ten or even fewer have been commercialized [51]. Furthermore, given that only carbohydrate components

Table 4. Comparative assessment of slow and flash pyrolysis of pine wood sawdust [61, 62]

Parameter	Slow pyrolysis	Flash pyrolysis
Temperature °C	350	500
Feed heating rate, °C/min	0.1–10	10–100
Contact time	1–120 min	0.5–1 s
Particle size, mm	1–2	1–2
Yield of gas	>21	8
Yield of bio-oil	<31	75
Yield of biochar	48	17

of plant feedstocks are suited for biochemical conversion, the entire lignocellulosic biomass cannot be converted [52].

Although thermochemical conversion of biomass is inferior in selectivity due to secondary cracking and condensation reactions, these can be minimized by choosing appropriate process conditions [51]. Unlike the other existing approaches, thermochemical conversion requires neither pretreatment of feedstocks nor any catalysts to be used [53]. Therefore, thermochemical conversion of lignocellulosic biomass exceeds the other alternatives in terms of process performance.

Thermochemical conversion of biomass is classified into high-temperature (>300°C) methods such as combustion, pyrolysis, and gasification [29], and low-temperature (<300°C) methods such as torrefaction and hydrothermal liquefaction [54]. Although direct combustion is the simplest and, hence, the most common method for biomass utilization, its efficiency has never exceeded 15–20% [55].

Biomass gasification provides a higher efficiency and produces synthesis gas, a raw material extensively used on an industrial scale. However, gasification requires high temperatures (800–1300°C) and a more complex process design [53].

Torrefaction is a low-temperature process designed to produce high-quality solid chemicals from biomass at 200–300°C and atmospheric pressure. It eliminates disadvantages of biomass such as non-uniformity, low bulk density, hygroscopicity, and fibrous structure [56]. However, this method exhibits low yields of liquid fuels and individual monomers.

Hydrothermal liquefaction produces liquids with relatively low oxygen content (10 wt %) and a high heating value (30–35 MJ/kg), but requires high pressures (up to 35 MPa) to be applied, thus rendering the process metal-intensive [57]. Given the high viscosity and high acidity of the bio-oil produced by hydrothermal liquefaction [58], this product cannot be used as a fuel without additional high-temperature treatment *via* catalytic cracking or HDO [57].

Pyrolysis is the most universal technique for biomass processing that provides the highest performance and the lowest costs. These benefits are achievable mainly due to relatively mild process conditions—atmospheric pressure and moderate temperatures (400 to 600°C)— and the high yield of desired bio-oil products (up to 75 wt %, depending on the process design and equipment arrangement) [59]. In chemical terms, biomass pyrolysis involves a combination of depolymerization, decarbonylation, and decarboxylation reactions that occur at high temperatures in the absence of oxygen [35]. Bio-oil is a mixture of defragmentation products of cellulose, hemicellulose, and lignin, its specific composition depending on the feedstock type. The composition and yield of pyrolysis products depend on the type and size of the feedstock particles as well as on the process parameters such as temperature, heating rate, and the residence time of the feedstock in the reaction zone [60].

Based on contact time, current pyrolysis processes can be categorized into slow/intermediate (several minutes to several hours), fast (1–3 s), and instantaneous/flash pyrolysis (<1 s) [61]. Due to its short contact time of flash pyrolysis, the undesirable secondary decomposition of intermediate resins into gases and biochar are suppressed. Table 4 presents a comparative assessment of slow and flash pyrolysis, which clearly shows the effects of contact time on product yields. As shown, the high-performance flash pyrolysis provides an enhancement of bio-oil yield.

In addition to contact time, the heating rate of fine feedstock particles (which have low thermal conductivity)

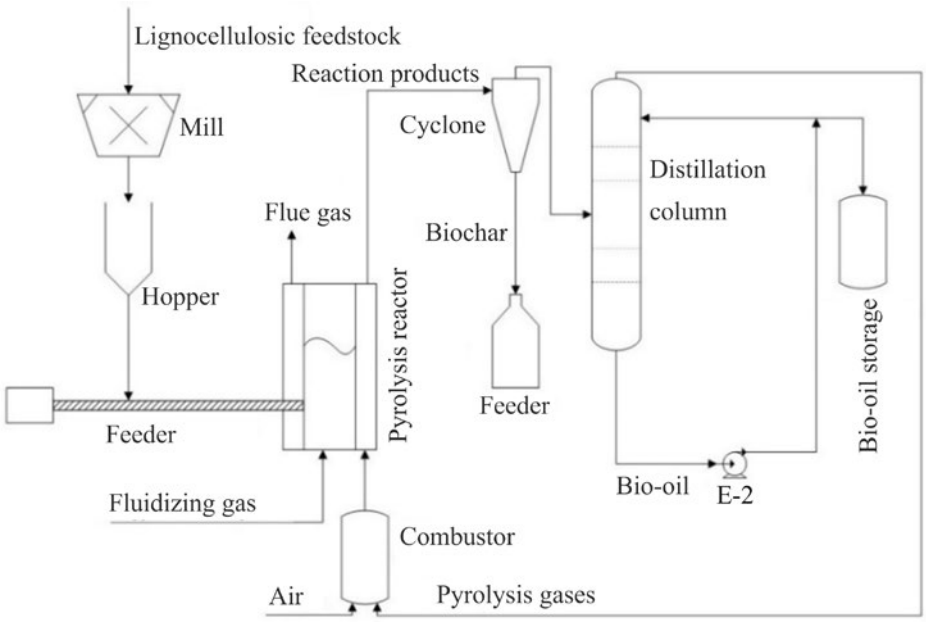

Fig. 1. Flow sheet for pyrolysis of lignocellulosic biomass in a fluidized bed reactor [45].

to a specific end temperature plays a major role. Relevant research has shown that the optimal size of feedstock particles is 1–2 mm [63].

The end temperature of the feedstock heating is critical to the pyrolysis process. Given the decomposition temperature range of 200–260°C for hemicellulose, 240–350°C for cellulose, and 280–500°C for lignin, the choice of process temperature is determined by the lignin content in the feedstock [64]. Lower pyrolysis temperatures promote the formation of biochar, whereas higher temperatures encourage cracking and result in increased gas yields. Thus, to maximize the yield of bio-oil, the pyrolysis temperature needs to be optimized for each specific feedstock type; for flash pyrolysis, the optimum temperature ranges between 400 and 600°C [65].

All the existing pyrolysis process designs use one common stepwise sequence. Initially, the feedstock enters a reactor and undergoes oxygen-free defragmentation at a high temperature, and the reaction mixture further flows to a separation section. On cooling, a portion of the reaction mixture condenses, and this liquid portion (bio-oil) is separated from the pyrolysis gas and the solid residue (biochar). The main existing types of pyrolysis reactors, as well as various methods for producing lignocellulosic bio-oil, are described below. Figure 1 shows a process design for lignocellulosic biomass pyrolysis in a fluidized bed reactor (FBR) [45].

FBR pyrolysis is one of the most common configurations for this process. This reactor type provides good heat and mass transfer, thus ensuring an isothermal bed for the reaction mixture [45]. One disadvantage of FBRs—a narrow range of contact time—can be eliminated by optimizing the particle size and gas flow rate, thus extending the time to 0.5–2 s. Another major disadvantage of a fluidized bed is the accumulation of large char particles in an upper bed which may act as a cracking catalyst increasing the yield of undesirable gas. Although fine-tuning of the granulometric composition of the feedstock helps overcome this challenge, it increases the feedstock cost. To solve this issue, the pyrolysis reactor design provides for the removal of char particles from the upper bubbling bed.

Figure 2 illustrates a schematic flow sheet for pyrolysis with a conical spouted bed reactor (CSBR) that has been developed as a modification of FBR pyrolysis [66].

One important advantage of this process design is cyclic movement of particles with a wide range of sizes, preventing their aggregation and accumulation as a char. Furthermore, the smaller dimensions of a CSBR, compared to other FBR types with equal output rates, reduce the capital costs. When implemented for flash

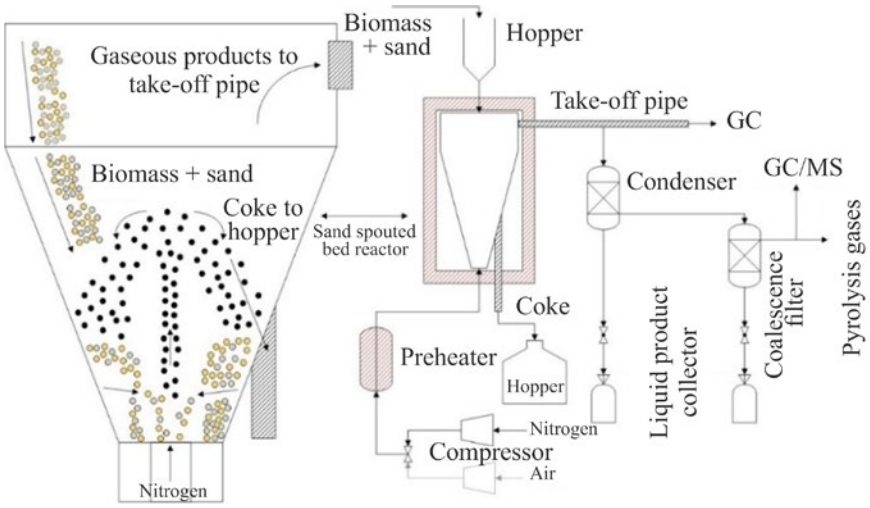

Fig. 2. Flow sheet for pyrolysis of lignocellulosic biomass in a conical spouted bed reactor [66].

pyrolysis, this promising CSBR technology has achieved high yields of bio-oil (71–75 wt %).

The University of Twente, the Netherlands, and Biomass Technology Group B.V. have developed a design for ablative pyrolysis (referred to as a BTG process) using a conical reactor [67]. The advantages of this technology are a stable bio-oil yield of about 70 wt % and the absence of a carrier gas (a design feature that facilitates product separation). However, commercial implementation of this process is complicated by certain upscaling challenges.

A number of other potential thermochemical conversion options of thermochemical biomass conversion, such as screw reactor, microwave, solar, vacuum, and plasma pyrolysis, have also been described [67–70]. To date, however, they either have not been developed further than laboratory testing or have never come close to the high bio-oil yields achieved by the methods discussed above. Table 5 summarizes the main characteristics of biomass pyrolysis for different feedstock types and process designs. These data clearly show that fast and flash pyrolysis have achieved the highest yields of bio-oil.

COMPOSITION AND MAIN REFINING ROUTES OF BIO-OIL

Lignocellulosic biomass (LCB) is the most sought-after type of renewable plant raw materials. LCB does not compete with food as a source for fuels and chemicals; it also contributes to the reduction of CO_2 emissions and ranks first in terms of reserves among sources of plant raw materials [77]. The crude bio-oil derived from LCB pyrolysis is of greatest interest because it can be

Table 5. Characterization of plant-based feedstock pyrolysis types

Feedstock	Pyrolysis type	Reactor type	*T*, °C	Yield of bio-oil, wt %	References
Waste furniture sawdust	Fast	FBR	450	65	[71]
Pine wood sawdust	Flash	CSBR	500	75	[62]
Pine wood sawdust	Fast	Screw	450	50	[72]
Softwood and hardwood pellets	Slow	Tubular vacuum	450	55	[73]
Sawdust	Fast	Cyclone	650	74	[73]
Wood waste	Fast	Circulating fluidized bed	500	40	[74]
Potato peel	Slow	Fixed bed	550	27	[75]
Corn cobs/stover	Fast	Circulating fluidized bed	650	62	[76]

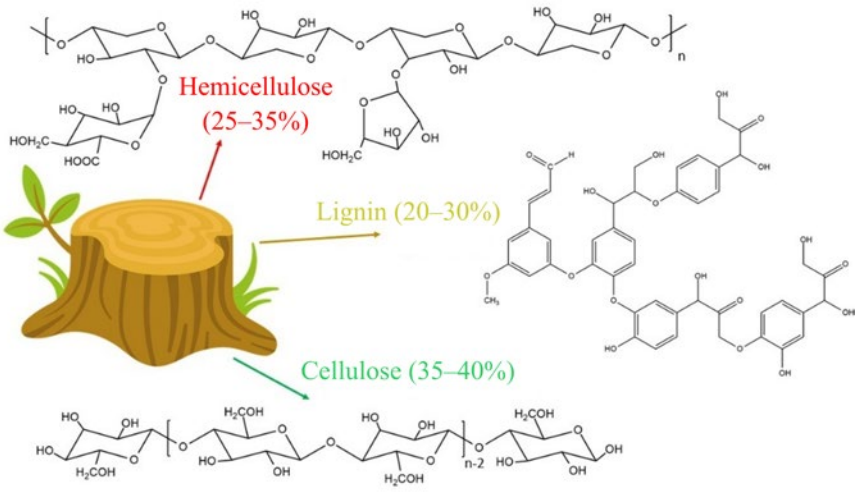

Fig. 3. Main components of lignocellulosic biomass.

used to produce liquid fuels or individual monomers [78]. Bio-oil is a complex mixture of more than 300 components, predominantly oxygenates. The pyrolysis product composition depends on the feedstock type as well as on the ratio of three main feedstock components, specifically cellulose, hemicellulose, and lignin (Fig. 3). The gross formulas of cellulose ($C_6H_{10}O_5$) and lignin ($C_{31}H_{34}O_{11}$) clearly reveal the significant difference in their compositions: appreciably higher concentrations of hydrogen and oxygen in the cellulosic components (C/H = 0.6 and 49.4%, respectively) than in lignin (C/H = 0.9 and 30.3%, respectively). Moreover, the cellulosic and lignin components differ in their stability. The overall composition of bio-oil can be identified through appropriate analysis by examining the degradation of each component.

Thermal degradation of cellulose can be described by two reaction types: gradual defragmentation, and charring with partial gasification at higher temperatures [79]. Cellulose initially decomposes into glucose, followed by dehydration of glucose into levoglucosan, which in turn undergoes a series of chemical transformations (Fig. 4). The final products of cellulose pyrolysis are levoglucosan, furan, furfural, acetic acid, acetone, and some other compounds [80].

Hemicellulose decomposes at a lower temperature and has a lower molecular weight than cellulose; furthermore, unlike cellulose, hemicellulose has a branched structure. The main component of hemicellulose is xylan, a compound that decomposes into water, methanol, formic acid, acetic acid, propionic acid, hydroxy-1-propanone, hydroxy-1-butanone, and furfural [81].

The most stable component of LCB is lignin, in which monomeric units are linked both by ether and strong C–C bonds. The lignin structure principally consists of three substituted phenols: sinapyl alcohol, coniferyl alcohol, and *p*-coumaryl alcohol (Fig. 5). During biomass pyrolysis, lignin is mostly defragmented into syringol, guaiacol, pyrocatechol, cresol, phenol, and their derivatives. Among the lignin degradation products that have been identified to date, phenols are the most common class: they account for more than 50 wt % [35, 82]. Kibet et al. [83] found that, in flash pyrolysis carried out within the range of 200–900°C, significant amounts of benzene, styrene, and *p*-xylene are also produced.

Importantly, lignin is the largest source of aromatic compounds on earth and the second (after cellulose) most abundant renewable source of carbon. In addition to conventional use for the production of surfactants, stabilizers, and epoxy resins, it has become increasingly worthwhile to produce individual aromatics and components of automotive and jet fuels from lignin.

Note that bio-oil has relatively small HC content, its predominant components being phenols, alcohols, and acids. The high oxygen content in bio-oil (up to 40 wt %) causes its high viscosity (6.2–7.0 mm^2/s), thermal and

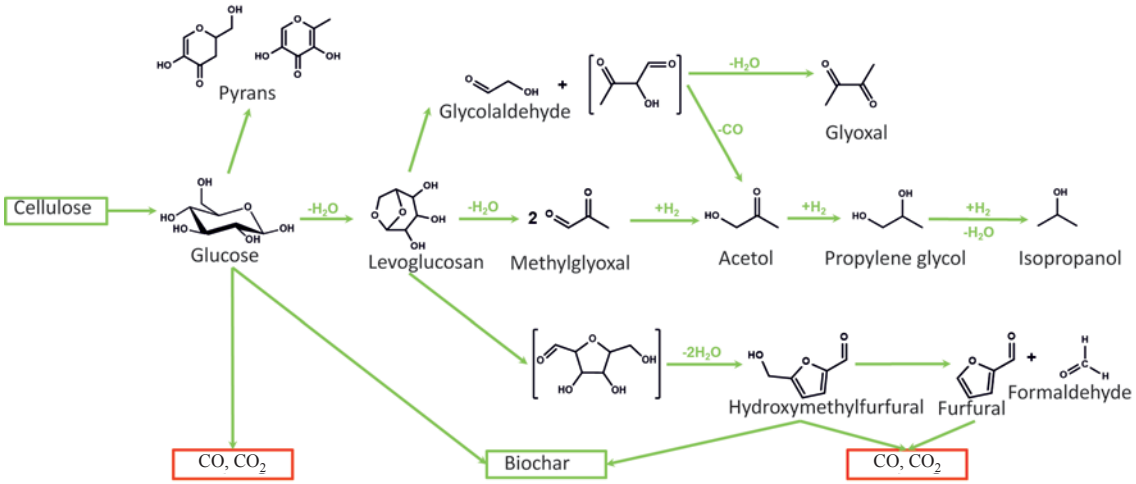

Fig. 4. Cellulose pyrolysis reactions.

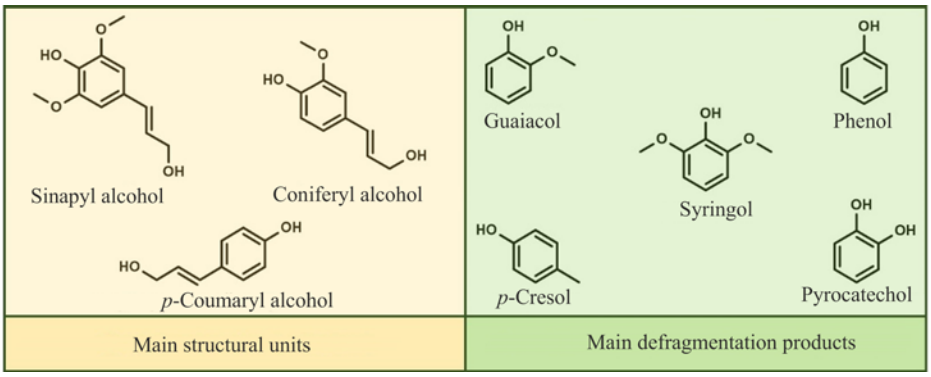

Fig. 5. Main structural units and defragmentation products of lignin.

chemical instability, high acidity (pH 2–3), and low energy density (20 MJ/kg).

Bio-oil applications include: its conversion to lighter products *via* catalytic cracking [84, 85], hydrotreating [86], or aqueous medium hydrogenation [87]; and production of high value-added individual chemicals.

The discussion below focuses on the upgrading of oxygenate components of bio-oil into HDO products. This upgrading solves the bio-oil utilization issue [67, 88] because the resultant products, including cyclohexane, cyclohexanol, phenol, benzene, toluene, etc., can be used as fuel components, as well as raw materials for the production of polyethylene terephthalate (PET), capron, nylon, and other large-scale petrochemicals [72]. The flow sheet of commercial biomass conversion into fuel fractions consists of two process sections: flash pyrolysis of biomass (described above) and biorefining of the bio-oil product (Fig. 6) [40].

The first biorefining step is pre-HDO of esters and acids at 200–300°C to facilitate downstream processing and transportation of the bio-oil [89]. Next, the partially upgraded product is subjected to complete HDO at 250–450°C and an increased hydrogen pressure (7.5–30 MPa) in the presence of heterogeneous catalysts. After dehydration, the product enters a distillation section to be separated into narrower fractions, namely gasoline, kerosene, diesel, and gasoil distillates as well as a heavy residue (fuel oil). To enhance the bio-oil conversion degree and produce additional amounts of lighter fractions, the residue is sent to hydrocracking or fluid catalytic cracking (FCC) [90].

Co-processing of plant and fossil feedstocks holds promise. This process design minimizes capital investments

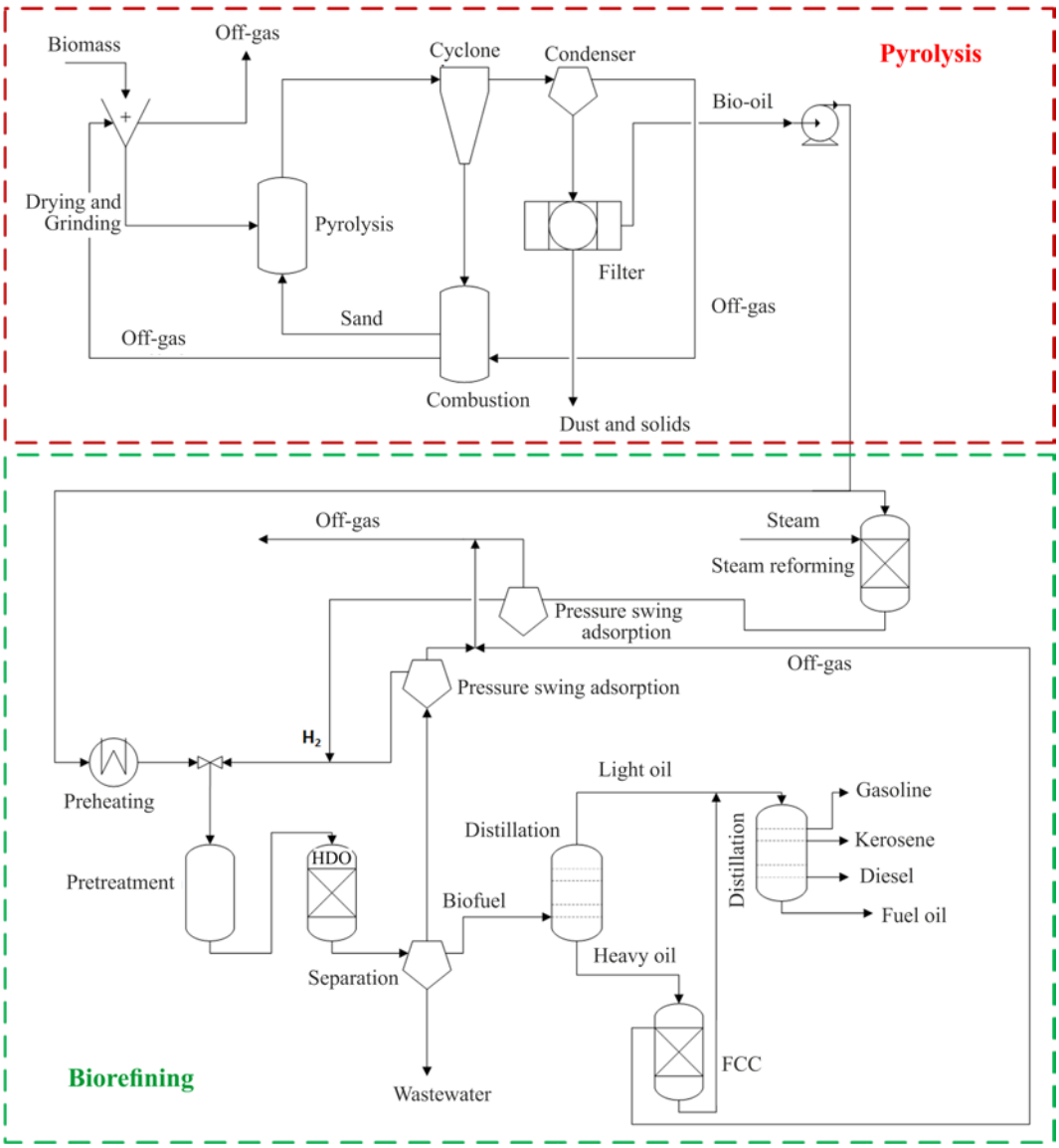

Fig. 6. Overall flow sheet for production of biofuels from LCB.

for bio-oil refining by integrating renewable feedstocks into existing refineries. For example, Domine et al. [85] report on FCC facilities operating under usual process conditions (450–530°C, WHSV 3–5 h^{-1}) with 2 wt % of bio-oil being added to vacuum gasoil. The zeolite catalyst was shown to remain active over at least ten reaction–regeneration cycles. However, increasing the bio-oil addition caused irreversible deactivation of the FCC catalyst due to polycondensation of lignin moieties and, hence, carbonaceous depositions on the catalyst.

To summarize the above discussion, it is fair to state that HDO is a promising technique for reducing the oxygen content in lignocellulosic bio-oil. HDO improves physicochemical properties of bio-oil such as viscosity and energy density, as well as reduces its acidity and oxygen content. The main problem of future researches would be the optimization of HDO process. An appropriate choice of an active, stable, and at the same time affordable HDO catalyst will allow cellulose- and lignin-derived products to be effectively integrated into existing fuel and chemical production facilities.

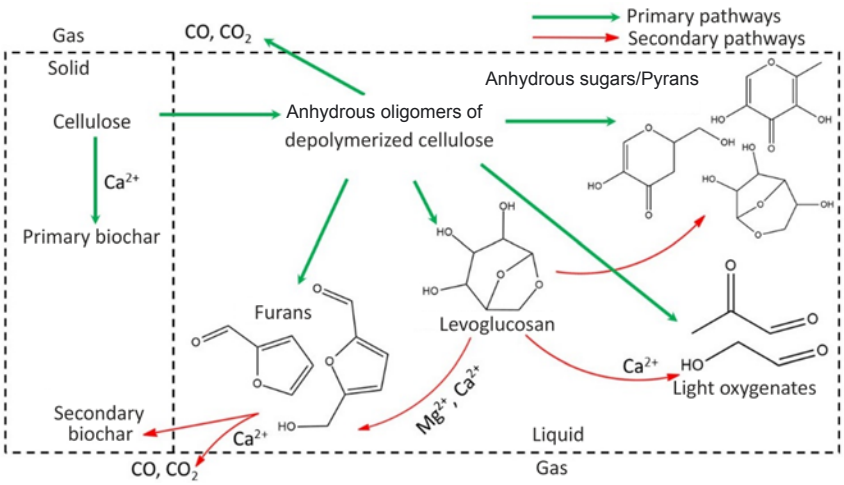

Fig. 7. Cellulose pyrolysis in the presence of Ca^{2+} and Mg^{2+} [80].

EFFECTS OF IMPURITIES ON PROCESSING OF PLANT BIOMASS

Processing of lignocellulosic raw materials is known to be strongly affected by the content of alkali and alkaline earth metals in the feedstock. Plant biomass always has some content of the nitrates and oxides of calcium, magnesium, and potassium, as well as various compounds of zinc and other metals [60, 80, 91]. Zhu et al. [80] investigated the effects of oxides and cations of calcium and magnesium present in the lignocellulosic feedstock on the yield of the cellulose pyrolysis products. Calcium was found to facilitate the primary charring of cellulose as well as secondary reactions that produce light oxygenates (glycol aldehyde and 2,3-butanedione) and carbon oxides. Magnesium, a metal with lower catalytic activity, mostly promotes secondary charring (Fig. 7). It was noted that increasing the content of calcium and magnesium results in higher yields of biochar and lower yields of bio-oil. Thus, in the case of highly mineralized feedstocks, it is preferrable to water-wash biomass in order to remove natural salts [81].

An aspect of equal importance is the effect of water, nitrogen-, and phosphorus-containing compounds present as impurities on the HDO of bio-oil. A high concentration of water in the bio-oil limits the application range of conventional hydrotreating catalysts and, in particular, the effective options for the active catalytic phase.

The hydrogen sulfide that forms during the decomposition of the sulfur compounds naturally present in the hydrotreating feedstock ensures the stability of sulfide catalysts. Water contained in bio-oil competes with hydrogen sulfide for adsorption on MoS_2 active sites, thus markedly diminishing the activity of sulfide catalytic systems [92]. Active sites of nickel-based catalysts are likewise poisoned with water. Moreover, water is able not only to adsorb on active sites but also to alter the catalyst's chemical structure. For example, on testing anisole HDO over NiP/SiO_2 and $NiMoP/SiO_2$ catalysts, Li et al. [93] found that water, which formed as a by-product, oxidized the NiP catalyst. The resulting nickel oxides and phosphates are known to be less active compounds than phosphides. Mortensen et al. [94] also reported on the negative effects of water. They observed that the presence of water in the model feedstock led to the deactivation of the $NiMoS_2/ZrO_2$ catalyst due to sulfide-to-sulfate oxidation at the edge of the MoS_2 active phase.

Apart from deactivating the active phase, water adversely effects alumina used as a support in hydrotreating catalysts. At 340–380°C, under the effect of water vapors, the alumina was converted to boehmite, thus resulting in the degradation of the support.

Likewise, nitrogen- and phosphorus-containing compounds negatively effect on bio-oil HDO due to poisoning active catalytic sites. Therefore, the factors most critical for HDO performance are the type of bio-oil precursor and the concentration of undesirable components. For example, microalgal biomass is rich in nitrogen, and phosphorus compounds have mainly been identified in leafy biomass. Bio-oil derived from wood

biomass has a noticeably lower nitrogen content, and no traces of phosphorus being detected at all [95–97].

Thus, the content of impurities in the lignocellulosic feedstock is what largely motivates the choice of the processing method, including the catalyst that would prove most effective in HDO.

CATALYSTS FOR HDO OF LIGNOCELLULOSIC BIO-OIL

To ensure effective processing at existing refineries, the bio-oil properties must satisfy the following requirements: low acidity (base number must not exceed 15 mg KOH/kg); high heating value (35–40 MJ/kg); low water content (0.1 wt % at highest); and complete miscibility with hydrocarbon fractions [3]. To meet these requirements, the bio-oil must be subjected to the catalytic HDO. Given that the HDO of bio-oil involves a combination of hydrogenation, isomerization, dehydration, and hydrogenolysis of oxygenates, the bifunctional catalysts comprising active metal sites on acid supports must be used [10, 98].

The active metal phase is involved directly in the hydrogenation of aromatic rings and in the saturation of multiple bonds [99]. Furthermore, the metal phase may be active in deoxygenation *via* direct hydrogenolysis of C–O bonds [100].

Oxides (e.g., ZrO_2, CeO_2, Al_2O_3, and TiO_2), carbon, zeolites (e.g., ZSM-5, Y, Beta, and SAPO-11), and mesoporous silica-based materials (e.g., SBA-15 and MCM-41) have been most commonly used as supports for the active phase (which is generally represented by metals or bimetallic composites) [10, 100, 101]. In the case of bifunctional catalysts, the support not only serves for the dispersion and stabilization of the active phase but also directly participates in catalysis due to the presence of Brønsted and Lewis acid sites (BAS and LAS, respectively) [98,102].

TThe activity and selectivity of bio-oil HDO catalysts largely depend on the active phase type, as well as on the acidity of the support and the size and geometry of its pores and channels.

Type of active metal phase in HDO catalysts. Bio-oil HDO catalysts can be divided into three main types [103]:

—conventional sulfided systems (e.g., $NiMoS/Al_2O_3$, $CoMoS/Al_2O_3$, and $Ni\text{-}WMoS/Al_2O_3$);

—catalysts based on transition metals (e.g., Ni, Zn, Cu, Fe, and W), including bimetallic catalysts; and

—catalysts based on noble metals (e.g., Pt, Pd, Ru, and Rh).

The use of sulfided catalysts faces a number of challenges [104]. Their active sites located at the MoS2 edges require a sulfurizing agent to be present in the reaction medium to ensure sustainable catalytic activity; however, this contaminates both reactants and products. Furthermore, sulfided catalysts in HDO release hydrogen sulfide, which inhibits the hydrogenolysis of methylphenols [105], thus decreasing the yield of high-octane aromatics (namely benzene, toluene, and xylenes). Another disadvantage of sulfided catalysts is the rapid deactivation due to coking [106, 107]. The increase of water concentration in the reaction medium has been found to retard the formation rate of both hydrogenation and deoxygenation products [108], which is especially typical of the sulfide form of a $Ni–Mo/\gamma\text{-}Al_2O_3$ catalyst [109]. Consequently, it is fair to state that sulfided catalysts are not optimal for bio-oil HDO.

A number of papers report on the use of catalysts based on transition metals (e.g., Ni, Zn, Cu, Fe, Co, Mo, and W), including bimetallic systems (Ni–Mo, Ni–Cu, Co–Mo, and Ni–Fe), in the HDO of lignocellulosic bio-oil [110, 111]. Among them, nickel catalysts are the most common: they have exhibited high activity in the hydrogenation of aromatic rings with high yields of cycloalkanes [112] and in the hydrogenolysis of C–O bonds of alcohols, ethers, and esters [113].

Figure 8 illustrates a two-step mechanism of the HDO suggested for phenol over the Ni/ZrO2 catalyst. The first step involves heterolytic dissociation of O–H bonds in phenol molecules with the formation of reactive phenoxide ions, $C_6H_5O^-$ [115, 116]. Simultaneously, the adsorbed hydrogen promotes the hydrogenation of the aromatic ring on the surface of nickel nanoparticles [117]. In the case of phenol, the hydrogenation occurs via formation of cyclohexanone, which is rapidly converted to cyclohexanol and, thus, remains only in negligible concentrations in the reaction products (the yield of cyclohexanone does not exceed 1.7 wt % [114]). The deoxygenation step involves hydrogenolysis directly on the surface of metallic nickel. As a result, cyclohexene is formed which is rapidly hydrogenated to cyclohexane—final product of the HDO.

In this case, the lower electrophilicity of metallic nickel—compared to other metals such as molybdenum or tungsten—results in its lower adsorption capacity with

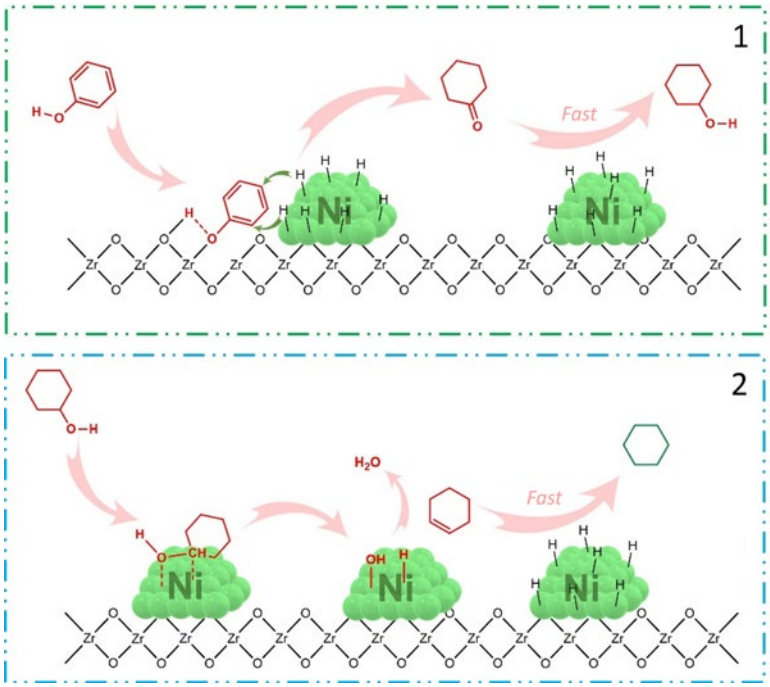

Fig. 8. Presumable mechanism for phenol HDO over Ni/ZrO_2 [114].

respect to oxygen-containing groups. Therefore, adding electrophilic components (e.g., Cu, Mo, W, Co, or Fe) to the catalyst enhances the electrophilicity of nickel atoms *via* a decrease in their electron density [118, 119]. In this context, Cu–Ni bimetallic catalytic systems have turned out to be the most efficient. In fact, according to the band theory, group IB metals such as copper have a completely filled *d*-sublevel, whereas group VIII metals such as nickel have a free *d*-orbital. Substitution of nickel atoms for copper in the crystalline framework increases the *d*-orbital filling degree, thus decreasing the concentration of adsorbed hydrogen and enhancing the HDO selectivity [120, 121]. Guo et al. [122] demonstrated that substitution of 40 wt % Ni for Cu provided the highest efficiency in the HDO of pyrolytic bio-oil, but further increasing the Cu content caused a deficiency in adsorbed hydrogen and decreased the catalytic activity.

Ni–Mo systems on acidic supports have also been considered efficient bimetallic catalysts for HDO [110]. Due to their especially high thermal stability and acid resistance, Ni–Mo alloys are well-suited for the HDO of acidic (pH 4–5) lignocellulosic bio-oil [123]. At moderate temperatures (300–400°C), Ni–Mo catalysts have exhibited high selectivity (up to 90%) towards saturated HCs; at higher temperatures (>400°C), hydrogenolysis of C–O bonds prevails with aromatic rings being retained [124].

In the HDO of lignocellulosic bio-oil, the stability of Ni-based catalysts is the main issue that has so far hampered their extensive use. The deactivation of Ni-based catalysts is mostly caused by coking, poisoning, sintering, and leaching of the active phase.

Coke formation has commonly been attributed to the acidic nature of the HDO catalyst support. For example, Vajglová et al. [125], who tested the HDO of isoeugenol and dihydroeugenol over a Fe–Ni/H-β catalyst at 300°C, report on a 4-fold and 2.3-fold conversion drop, respectively, after 1 h of reaction. At that time, 18% of coke was deposited on 99% of the catalyst surface. The formation of coke and its precursors (e.g., biphenyl, anthracene, and phenanthrene) has also been observed at higher temperatures (410°C) in anisole HDO over a catalyst on an inert support, $Ni–Mo/SiO_2$ [126].

Active catalytic sites may be poisoned as a result of the adsorption of so-called catalytic poisons on the catalyst surface. In the HDO of lignocellulosic bio-oil, initial reactants, intermediates, and product impurities may act as catalytic poisons. For example, the water that forms during HDO tends to compete with feedstock components for adsorption on active catalytic sites.

Li et al. [127] show that, in anisole HDO over NiP/SiO_2 and $NiMoP/SiO_2$, water leads to the oxidation of NiP to nickel oxide, a compound inferior to nickel phosphide in catalytic activity.

Another important challenge, especially exacerbated with a temperature rise, is the susceptibility of the active phase of Ni-based catalysts to sintering. Argyle and Bartholomew [128] demonstrate, for the case of *o*-cresol HDO over a $Ni/SiO_2–Al_2O_3$ catalyst, that sintering of nickel resulted in the enlargement of nickel crystallites from 3.8 to 36 nm.

Some researchers have reported on the leaching of the active phases of Ni-based catalysts in the HDO of lignocellulosic bio-oil. In testing the phenol HDO, Zhao et al. [129] detected that nickel was leached from a Ni/Al_2O_3–ZSM-5 catalyst at 200°C and a hydrogen pressure of 5 MPa, thus decreasing the HC selectivity from 70 to 25%. Dickinson and Savage [130] found, for the case of *o*-cresol HDO over a $Ni/SiO_2–Al_2O_3$ catalyst, that both the activity and deoxygenation degree dramatically dropped due to leaching aluminum and enlargement of nickel crystallites.

Catalysts based on noble metals such as Pt, Pd, Rh, Ru, and Ir have exhibited high activity in the HDO of lignocellulosic feedstocks [131–133]. Unlike conventional sulfided systems, these catalysts do not require sulfiding agents and allow liquid-phase HDO to be implemented under mild conditions [134]. Furthermore, noble-metal catalysts are distinguished by increased dispersion of the active phase and high resistance to leaching by acidic bio-oil components [135]. Although all the above-mentioned challenges that affect the HDO catalyst stability are valid for noble-metal catalytic systems as well, these systems have achieved a greater stability and activity in the HDO of lignocellulosic bio-oil.

Wildschut et al. [136] compared the activity of sulfided NiMo and CoMo catalysts with a variety of noble-metal catalysts (Pt/C, Pd/C, Ru/C, Ru/TiO_2, and Ru/Al_2O_3) at 350°C and 20 MPa after 4 h of reaction. The yield of liquid organics ranged from 25 to 67 wt %, reaching its maximum in the presence of Ru/TiO_2. The highest oxygen content (11 wt %) was observed for the sulfided $NiMo/Al_2O_3$ catalyst and the lowest (6 wt %) for Ru/C. The Ru/C catalyst was more attractive due to minimal yield of gaseous products (6 wt %). Unfortunately, the common disadvantage of all noble-metal catalysts is their high cost.

Among noble-metal catalysts, mono- and bimetallic systems based on palladium and/or platinum have been used most extensively [137–139]; they have proven highly active in hydrogenation. The HDO of bio-oil's phenolic components over platinum-group metals occurs preferentially *via* the saturation of aromatic rings and the hydrogenolysis of C–O bonds. Acidic supports such as Al_2O_3, aluminosilicates, and zeolites, have enabled researchers to synthesize bifunctional catalysts highly active in deoxygenation [140].

Palladium catalysts have often been used in the HDO of lignocellulosic bio-oil: they activate direct hydrogenation of aromatic or furan rings prior to C–O cleavage [141–144]. This HDO route is initiated not only due to the high hydrogenation activity of these catalysts but also because palladium interacts more strongly with the aromatic ring than with the C–O or C=O groups [145]. Ardiyanti et al. [146] found that the Pd/ZrO_2 catalyst exhibits a higher activity in bio-oil HDO than Pt/ZrO_2. However, Pd-based catalysts are more susceptible to deactivation due to coking than their Pt-based counterparts [147]. Bimetallic Pd–Fe catalysts have exhibited high performance in the production of aromatics by HDO: they promote hydrogenolysis of the C–O bond without affecting the aromatic ring [131].

Ruthenium-based supported catalysts have also turned out to be highly active in the HDO of model components of lignocellulosic bio-oil [114, 147–149]. A comparative assessment of the catalytic activity of Pt-, Pd-, and Ru-based systems in phenol HDO has demonstrated the superiority of the ruthenium-based samples [114]. Roldugina et al. [148] investigated the activity of Ru catalysts supported on mesoporous aluminosilicate Al-HMS(10) in guaiacol HDO between 200 and 300°C. Heating was shown to promote more complete conversion of guaiacol and enhance the yield of aromatics. When the HDO temperature was elevated to 300°C, pyrocatechol, phenol, and cresol appeared in the reaction products.

Given the bifunctionality of HDO catalysts, their supports are important for deoxygenation [150]. The most promising supports are aluminosilicates having BAS and LAS sites, such as zeolites (ZSM-5, Y, Beta, SAPO-11), mesoporous silicas (SBA-15, MCM-41, HMS), alumina, and some other materials [12, 102, 140, 150–153]. Kinetic studies of model bio-oil components are of importance to gain a better understanding of the chemistry and regularities of HDO over bifunctional catalysts [154–156]. In the eugenol HDO, Bjelić et al. [154] have performed the most detailed kinetic analysis of the process. This enabled them to thoroughly investigate

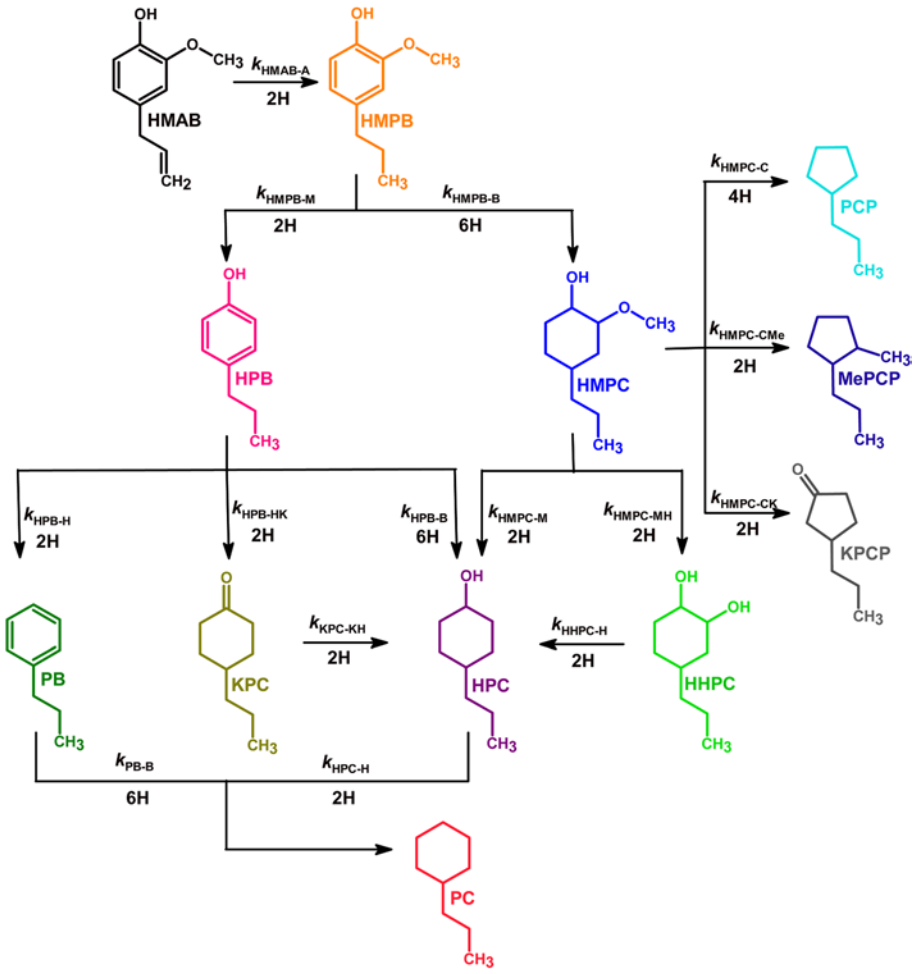

Fig. 9. Eugenol HDO reactions over Pt/C, Pd/C, Rh/C, Ru/C, Ni/C, and Cu/C catalysts. Denotations: (HMAB) Eugenol; (HMPB) 2-methoxy-4-propylphenol; (HPB) 4-propylphenol; (HMPC) 2-methoxy-4-propylcyclohexanol; (PCP) propylcyclopentane; (MePCP) 1-methyl-3-propylcyclopentane; (KPCP) 3-propylcyclopentanone; (PB) propylbenzene; (KPC) 4-propylcyclohexanone; (HPC) 4-propylcyclohexanol; (HHPC) 4-propylcyclohexanediol-1,2; and (PC) propylcyclohexane.

the physicochemical properties and catalytic performance of Pt/C, Pd/C, Rh/C, Ru/C, Ni/C, and Cu/C, as well as to provide a schematic diagram of eugenol transformations comprising 11 reaction steps (Fig. 9).

This study further provides a kinetic characterization of all the reaction steps and a calculation of the related rate constants and activation energies. The hydrogenation of the aromatic ring was shown to be approximately 3-, 11-, 32-, 10-, and 6-fold faster than the C–O hydrogenolysis over Ru, Pt, Pd, Rh, and Ni, respectively. Methoxy and hydroxy groups were found to be more easily removed from aromatics than from naphthenes. Among the catalysts under study, Ru/C exhibited the highest performance in the conversion of eugenol to hydrocarbons. This was due to the optimum balance of its activity between the aromatic ring hydrogenation and the C–O hydrogenolysis.

Oxygen removal can be induced not only by hydrogenolysis but also by protonation on acid sites. The acidity of the support has a major effect on the product distribution *via* activation of the dehydration, hydrogenation, isomerization, and (partially) cracking of the oxygenated feedstock [157]. An equally important property of supports is the presence of a developed system of pores and channels that facilitates the diffusion of reactants toward active sites. Therefore, the discussion below focuses on the effects of the type and properties of micro–mesoporous aluminosilicate supports on the performance of reactions that involve the oxygenated compounds of bio-oil.

Micro–mesoporous aluminosilicate for bio-oil HDO catalysts: properties and prospects (Effects of the acidity of the support and the geometry and size of its pores and channels on catalyst properties). Deoxygenation reactions are known to be accelerated by acidic catalysts such as zeolites and aluminosilicates [158–160]. Therefore, bio-oil HDO process designs are generally based on using bifunctional catalysts that combine hydrogenation and acid sites. The activity and selectivity of these catalysts largely depend on the structure and acidity of their supports, most often zeolites.

As mentioned above, during HDO, oxygenates are hydrogenated on active metal sites, whereas the support performs acidic functions critical to the deoxygenation degree and to the generation pattern of the active metal phase.

Having great acidity and hydrothermal stability, ZSM-5-supported catalysts exhibit the highest activity in the hydrotreating of bio-oil components [150, 161, 162]. Ohta et al. [163] show that cycloalkanes can be produced in high yields up to 99% by the HDO of substituted phenols at relatively low temperature (383 K) and H2 pressure of 0.1 MPa using the Pt/ZSM-5 catalyst in a nonpolar solvent. However, this unstable catalytic system lost its activity after only two cycles.

Song et al. [164] investigated the HDO activity of the 20% Ni/ZSM-5 catalyst in mixtures of substituted phenols and guaiacol. Metallic nickel nanoparticles were found to play a key role in the hydrogenation of aromatics, whereas hydrolysis and dehydration occur on the support's acid sites. At 523 K and 5 MPa H_2, the yield of cycloalkanes was 73–92%, and that of aromatics and methanol reached 15%; the content of by-products did not exceed 18%.

Simultaneously, high concentrations of acid sites in ZSM-5 may intensify cracking reactions, thus decreasing the selectivity towards desired products and accelerating the coking of the catalyst [165]. Graça et al. [84, 166] tested the ZSM-5-supported catalyst in the HDO of phenol and guaiacol. They demonstrated that the increased acidity of the zeolite support led to intense coke formation and rapid catalyst deactivation due to the adsorption of phenolic compounds on acid sites followed by the blocking of catalyst micropores.

Zeolite acidity can be adjusted by altering the Si/Al ratio during the synthesis or by etching. Increasing the Si/Al ratio reduces the concentration of acid sites and, thus, slows the cracking and isomerization reactions [167]. Varying the concentration and ratio of acid sites in Pt catalysts supported on SAPO-11 and ZSM-22 affects their selectivity in bio-oil HDO, thus requiring a balance to be maintained between these sites [168]. Shafaghat et al. [169] studied the effects of adding ZSM-5 and Y zeolites with different Si/Al ratios on the catalytic activity and selectivity of the Pd/C catalyst in the HDO of phenol, o-cresol, and guaiacol. The addition of ZSM-5 with Si/Al = 80 to the Pd/C catalyst boosted the phenol conversion from 48 to 97%, whereas the addition of ZSM-5 with Si/Al = 30 had virtually no effect on the phenol conversion.

Besides the balance between acid sites, another factor of importance in the HDO of bio-oil is the microporous zeolite structure. The main disadvantage of microporous materials is their diffusion limitation that arises from the adsorption/desorption of substrate/product molecules those kinetic diameters exceeds the pore diameter of zeolite. This hinders the access to active sites for the reactant molecules and decreases the feedstock conversion [170]. In the HDO of phenols, wide-pore zeolites Pt/Y and Ni/Beta provide adequate accessibility to active metal sites for guaiacol molecules and exhibit a higher activity than Pt-meso-MFI [171] and Ni/ZSM-5 [172]. The lower activity of ZSM-5 can be explained by diffusion hindrances for guaiacol molecules inside this microporous zeolite [150]. Compared to the ZSM-5-supported catalyst, Ru/meso-MFI exhibited excellent activity and selectivity towards saturated HCs due to the accessibility of acid sites in the large mesopores of MFI [173]. A similar effect was reported in the cases of meso-MFI used for Ni [174] and Pt catalysts [175].

The above discussion obviously suggests good prospects for using MCM-41, SBA-15, HMS, and some other mesoporous materials in the HDO of oxygenated components of bio-oil [98, 148, 176]. The silica-based materials specified have a high specific surface area (about 1000 m2/g) and a narrow pore size distribution with a maximum in the mesopore region (2–10 nm). These properties are responsible for high dispersion and good accessibility of metal and acid sites to feedstock molecules [177, 178]. For example, the dispersion of Rh particles supported on MCM-41 was higher than that of zeolite-supported Rh [179]. The micropore diameter of the zeolite catalysts turned out to be insufficient for the incorporation of rhodium nanoparticles—in contrast to the MCM-41 silica mesopores well suited for the deposition of metal particles. Moreover, the ordered hexagonal mesopores (d = 2.7 nm) in MCM-41 ensured

Table 6. HDO of lignocellulosic bio-oil in presence of catalysts supported on MCM-41 mesoporous silica

Catalyst	T, °C	$P(H_2)$, atm	Feedstock	Conversion, %	Main products (in descending order of yield)	References
Fe/MCM-41	350	1	Guaiacol	3.6	Benzene, toluene	[186]
Ru/MCM-41	130	60	Anisole	70.0	Toluene, metoxycyclehexene	[187]
Pd/MCM-41	130	60	Benzophenone	74.0	Diphenylmethane, benzohydrole	[188]
Cu–Ni/MCM-41	260	100	Guaiacol	37.0	Cyclohexane, cyclohexanol	[98]
Cu–Ni/Ti-MCM-41	260	100	Guaiacol	91.5	Cyclohexanol, toluene	[98]
Ni/Al-MCM-41	400	1	Guaiacol	95.0	Methane, phenol	[102]
Ni/MCM-41	280	48	Anisole	39.0	Cyclohexane	[184]

a higher mass transfer rate than the zeolite-supported reference samples.

However, the low acidity of MCM-41-like materials (0.06–0.12 mmol/g) provides no opportunity for achieving a high degree of deoxygenation of lignocellulosic feedstocks [180]. One effective approach to overcome this challenge is to increase the acidity of supports by promoting them with metals such as Al, Ti, Nb, Zr, Ce, V, and Cr [98, 181, 182]. Incorporating Ti into mesoporous silica enabled Amburso et al. [98] to appreciably increase the concentration of acid sites, specifically from 0.119 mmol/g for MCM-41 to 5.573 mmol/g for Ti–MCM-41. Similar titanium promotion caused the substantial rise in activity and selectivity of the Cu–Ni/Ti–MCM-41 catalyst: the guaiacol conversion reached 91.5% and the cyclohexane selectivity was 50%, compared to 37 and 10.5%, respectively, for the Ti-free catalyst (Cu–Ni/MCM-41).

One of the most common techniques for enhancing the acidity of mesoporous siliceous materials is to incorporate aluminum into the support's framework [102, 183, 184]. Taghvaei et al. [185] describe the HDO of anisole over Ni/Al–MCM-41 catalysts with various Si/Al ratio (10, 20, 40, and 60). All the catalysts exhibited high activity and selectivity, with phenol and benzene being the main reaction products. The anisole conversion reached its maximum (64.2%) when the most acidic support (Si/Al = 20) was used. Under more rigorous process conditions, the anisole conversion on the Ni/Al–MCM-41 catalysts increased up to 97%. In this case, the main product was cyclohexane (95% yield), which is indicative of the high deoxygenation ability of the catalytic systems supported on mesoporous silica when aluminum is incorporated. Further increasing the aluminum content (Si/Al < 10) declines both the surface area and pore diameter of the support, thus decreasing the catalytic activity in the HDO.

Table 6 summarizes the available data of effects of the main HDO process parameters on the feedstock conversion and product distribution for various catalysts supported on MCM-41-type mesoporous silica.

Thus, in view of the high surface area, the ordered mesopores, and the adjustable acidity, mesoporous silica-based materials such as MCM-41 hold great promise to be used as supports in catalysts for the HDO of lignocellulosic bio-oil. However, the applicability of modern mesoporous silicas for high-temperature hydrotreatment is limited by two major drawbacks of these materials: low thermal stability (600–700°C) and low mechanical strength (190–220 MPa) [189]. One potential solution to this problem is to reinforce mesoporous silica with strong materials such as halloysite [190], a mineral that has great potential for catalysis, particularly, in the HDO of lignocellulosic bio-oil [191].

Halloysite nanotubes: unique properties and prospects. In recent years, aluminosilicate halloysite nanotubes (HNTs) have been increasingly used, both in the synthesis of individual supports [192, 193] and as a precursor for the synthesis of mesoporous molecular sieves [194, 195]. Halloysite is an aluminosilicate of the kaolin group with the chemical formula $Al_2Si_2O_5(OH)_4 \cdot nH_2O$ (n = 2) formed by rolling of aluminosilicate sheets into a hollow tube [196]. The tube dimensions and mineral microstructure are shown in Figs. 10a–10c.

HNTs have been extensively used as the catalysts for a variety of petrochemical processes such as isomerization of C_8 gasoline [197], selective hydrogenation of benzene (contained in naphtha reformate) [194], hydroformylation of alkenes [198], Fischer–Tropsch synthesis [199], and hydrodesulfurization of gasoline and diesel fractions

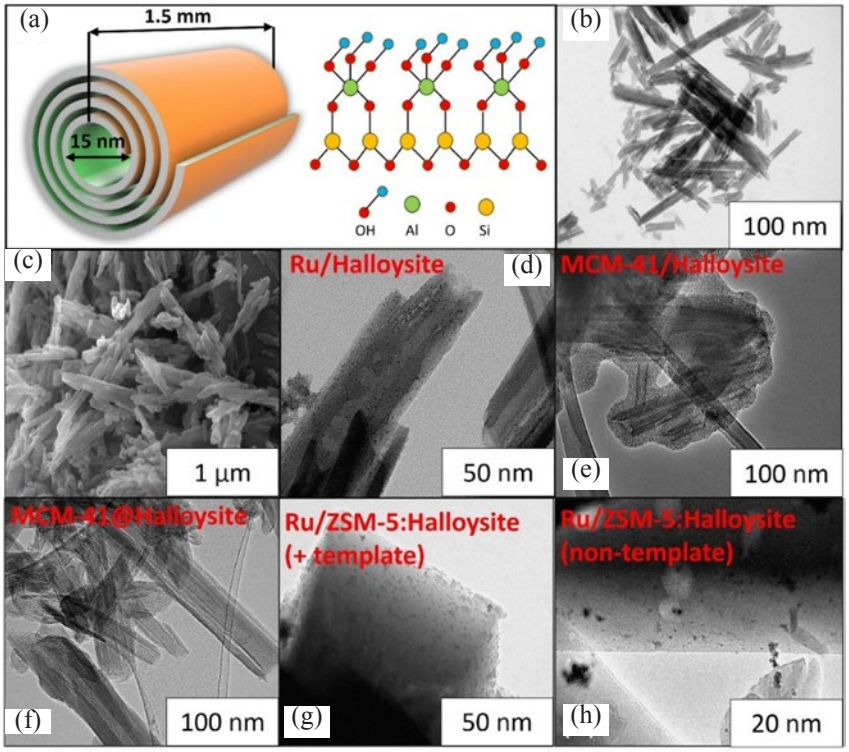

Fig. 10. Aluminosilicate HNTs and their micrographs: (a) halloysite morphology and structure; (b) TEM micrograph of halloysite; (c) SEM micrograph of halloysite; (d) TEM micrograph of Ru/ halloysite catalyst; (e) TEM micrograph of MCM-41/halloysite composite (mesoporous silica located around HNTs); (f) TEM micrograph of MCM-41@halloysite composite (mesoporous silica located inside HNT lumen); (g) TEM micrograph of Ru/ZSM-5:halloysite catalyst (templated); and (h) TEM micrograph of Ru/ZSM-5:halloysite catalyst (template-free).

[200, 201]. Previous study has demonstrated the effects of acid dealumination of halloysite on the activity of Ru/HNT catalysts as used in the HDO of lignocellulosic bio-oil [202]. Dealuminated halloysite was shown to have a high specific surface area of 154 m^2/g and moderate acidity of about 0.34 mmol/g. In the liquid-phase HDO of guaiacol, the ruthenium catalyst supported on dealuminated halloysite exhibited higher values of activity (TOF = 211 h^{-1}) and cyclohexane selectivity (15%) than the catalyst supported on pristine nanotubes. Serrano-Maldonado et al. [203] describe a series of Co/HNT catalysts active in the hydrogenation of alkenes, mono- and polyunsaturated fatty acids, and C_{18} esters. Zhang et al. [204] developed a halloysite-supported bifunctional catalyst for the depolymerization of cellulose into 5-hydroxymethylfuran.

Halloysite has proven to be an excellent support for a finely dispersed (1.5–5 nm) active metal phase mainly located on the external nanotube surface (Fig. 10d). Catalytic systems of this kind exhibit high activity in the hydrogenation of C_6–C_8 aromatics and phenol [205–208].

Modification of the halloysite surface with organosilane surfactants has enabled the development of catalytic systems that exhibit high activity and stability in corrosive media (e.g., phenolic water) [209]. In accordance with this approach, the active metal phase was mostly generated inside the lumen of the nanotubes, and the catalyst being concentrated in the hydrocarbon medium. As a result, the catalyst performance increased to TON 50 or even higher.

Another promising approach is to synthesize HNT-based composite supports (Figs. 10d–10h). For example, HNTs can be used to synthesize composites such as MCM-41/halloysite (with MCM-41 located on the external surface, Fig. 10e) or MCM-41@halloysite (with MCM-41 located inside the HNT lumen, Fig. 10f) [190, 210]. This approach makes it possible to obtain supports with a developed surface (S_{BET} = 400–600 m^2/g) and an active phase being immobilized into the

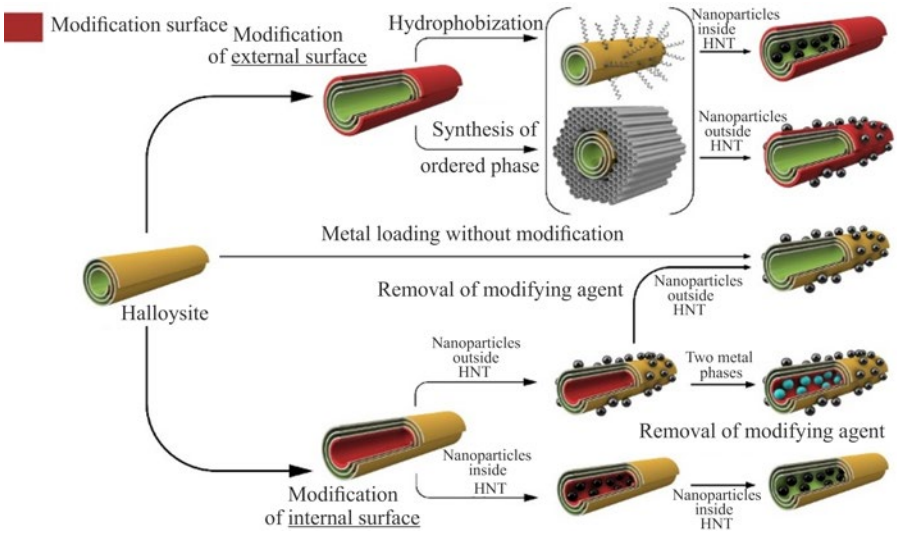

Fig. 11. Key strategies and approaches for modification of HNTs and synthesis of halloysite-based hierarchical materials [192].

well-developed hexagonal channels of MCM-41. In this system, halloysite generates secondary through-channels that ensure intense transport of molecules inside the pores.

Halloysite has further been used for modification of zeolite catalysts. As mentioned above, the microporosity and high acidity of zeolite-based systems limit their application in the HDO of lignocellulosic raw materials. The unique properties of a recently invented micro–mesoporous material have effectively overcomed these disadvantages [195]. This material was synthesized by introducing a mesoporous component during the hydrothermal synthesis of ZSM-5 from halloysite, either with a template or free (Figs. 10g, 10h). Such a zeolite synthesized has mesopores (5–6 nm) and relatively high content (0.413 mmol/g) of strong BAS (as identified by ammonia desorption in the region of 350–500°C), i.e., the acid sites responsible for the deoxygenation of oxygenates [211].

Figure 11 summarizes, in the form of schematic diagram, the most promising approaches for halloysite surface modification, as well as techniques for synthesizing new hierarchical composites.

CONCLUSIONS

The development of process design for the catalytic HDO of lignocellulosic bio-oil is of great importance both from the economic and environmental viewpoints. Involving renewable organic raw materials in the process chain would significantly diversify the range of fuels and allow high value-added chemicals to be produced. One major challenge that currently limits the expansion of production capacities for the HDO of lignocellulosic bio-oil is a lack of active catalysts resistant to sintering at high temperatures, to leaching by acidic components of bio-oil, and to deactivation in the presence of water.

Given the significant difference between the cellulosic and lignin components of lignocellulosic biomass in terms of hydrogen and oxygen content, it appears reasonable to separate these components in order to subsequently process them for fuel and petrochemical applications, as appropriate. Obviously, these different processing routes must occur under different process conditions in terms of temperature, hydrogen to feedstock ratio, water to feedstock ratio, and catalyst type. Therefore, the development of high-performance catalysts is one of the most urgent problems that face the processing of lignocellulosic biomass.

Unfortunately, to date research in this area has not advanced further than laboratory testing and proof-of concept. However, the high degree of interest on the part of many research teams and corporate centers worldwide clearly indicates that modern oil refining needs new catalysts to be developed. These catalysts must be active and stable in the processing and conversion of lignocellulosic feedstocks.

AUTHOR INFORMATION

G.O. Zasypalov, ORCID: https://orcid.org/0000-0001-9712-3717

V.A. Klimovsky, ORCID: https://orcid.org/0000-0002-3197-3003

E.S. Abramov, ORCID: https://orcid.org/0009-0002-8404-1581

E.E. Brindukova, ORCID: https://orcid.org/0000-0002-2294-5967

V.D. Stytsenko, ORCID: https://orcid.org/0000-0001-8782-2098

A.P. Glotov, ORCID: https://orcid.org/0000-0002-2877-0395

FUNDING

This study was funded by the Russian Science Foundation (project no. 23-29-00589, https://rscf.ru/project/23-29-00589/).

CONFLICT OF INTEREST

The authors declare no conflict of interest requiring disclosure in this article.

REFERENCES

1. Akinfiev, V.K., *Energ. Polit*., 2020, vol. 1, p. 143.
2. Makarov, A.A., Mitrova, T.A., and Kulagin, V.A., *Forecast for the Development of Energy and Russia 2019*, Moscow School of Management SKOLKOVO, 2019.
3. Topolyuk, Y.A., Nekhaev, A.I., and Zasypalov, G.O., *Oil Gas Chem*., 2021, no. 2, pp. 22–28.
4. Alonso, D.M., Wettstein, S.G., and Dumesic, J.A., *Chem. Soc. Rev*., 2012, vol. 41, no. 24, p. 8075. https://doi.org/10.1039/C2CS35188A
5. Yan, L., Yao, Q., Fu, Y., *Green Chem*., 2017, vol. 19, no. 23, pp. 5527–5547. https://doi.org/10.1039/C7GC02503C
6. Naranov, E., Sadovnikov, A., Arapova, O., Kuchinskaya, T., Usoltsev, O., Bugaev, A., Janssens, K., De Vos, D., and Maximov, A., *Appl. Catal. B: Environmental*, 2023, vol. 334, p. 122861. https://doi.org/10.1016/j.apcatb.2023.122861
7. Martone, P.T., Estevez, J.M., Lu, F., Ruel, K., Denny, M.W., Somerville, C., and Ralph, J., *Curr. Biol*., 2009, vol. 19, no. 2, pp. 169–175. https://doi.org/10.1016/j.cub.2008.12.031
8. Rakhmankulov, D.L., Vil'danov, F.Sh., Nikolaeva, S.V., and Denisov, S.V., *Bashkir. Khim. Zh*., 2008, vol. 15, no. 2, pp. 36–52.
9. Long, J., Shu, R., Yuan, Z., Wang, T., Xu, Y., Zhang, X., Zhang, Q., and Ma, L., *Appl. Energy*, 2015, vol. 157, pp. 540–545. https://doi.org/10.1016/j.apenergy.2015.04.011
10. Kay Lup, A.N., Abnisa, F., Wan Daud, W.M.A., and Aroua, M.K., *J. Indust. Eng. Chem*., 2017, vol. 56, pp. 1–34. https://doi.org/10.1016/j.jiec.2017.06.049
11. de Miguel Mercader, F., Groeneveld, M.J., Kersten, S.R.A., Way, N.W.J., Schaverien, C.J., and Hogendoorn, J.A., *Appl. Catal. B: Environmental*, 2010, vol. 96, nos. 1–2, pp. 57–66. https://doi.org/10.1016/j.apcatb.2010.01.033
12. Zhao, C. and Lercher, J.A., *ChemCatChem*., 2012, vol. 4, no. 1, pp. 64–68. https://doi.org/10.1002/cctc.201100273
13. Ennaert, T., Van Aelst, J., Dijkmans, J., De Clercq, R., Schutyser, W., Dusselier, M., Verboekend, D., and Sels, B.F., *Chem. Soc. Rev*., 2016, vol. 45, no. 3, pp. 584–611. https://doi.org/10.1039/C5CS00859J
14. Zhu, X., Mallinson, R.G., and Resasco, D.E., *Appl. Catal. A: General*, 2010, vol. 379, nos. 1–2, pp. 172–181. https://doi.org/10.1016/j.apcata.2010.03.018
15. Shafiee, S. and Topal, E., *Energy Policy*, 2009, vol. 37, no. 1, pp. 181–189. https://doi.org/10.1016/j.enpol.2008.08.016
16. Naik, S.N., Goud, V.V., Rout, P.K., and Dalai, A.K., *Renewab. Sustain. Energy Rev*., 2010, vol. 14, no. 2, pp. 578–597. https://doi.org/10.1016/j.rser.2009.10.003
17. Mittelbach, M., *Eur. J. Lipid Sci. Technol*., 2015, vol. 117, no. 11, pp. 1832–1846. https://doi.org/10.1002/ejlt.201500125
18. Sun, Y., Li, C., Li, Q., Zhang, S., Xu, L., Gholizadeh, M., and Hu, X., *J. Energy Instit.*, 2021, vol. 97, pp. 1–12. https://doi.org/10.1016/j.joei.2021.03.020
19. Vieira, F.R., Romero Luna, C.M., Arce, G.L.A.F., and Ávila, I., *Biomass Bioenerg*., 2020, vol. 132, p. 105412. https://doi.org/10.1016/j.biombioe.2019.105412
20. Tsarpali, M., Arora, N., Kuhn, J.N., and Philippidis, G.P., *Algal Res.*, 2021, vol. 57, pp. 102354. https://doi.org/10.1016/j.algal.2021.102354
21. Bechara, R., Gomez, A., Saint-Antonin, V., Schweitzer, J.-M., Maréchal, F., and Ensinas, A., *Renewab. Sustain. Energy Rev*., 2018, vol. 91, pp. 152–164. https://doi.org/10.1016/j.rser.2018.02.020
22. Tao, J., Yu, S., and Wu, T., *Biomass Bioenerg*., 2011, vol. 35, no. 9, pp. 3810–3829.

https://doi.org/10.1016/j.biombioe.2011.06.039
23. Norkobilov, A., Gorri, D., and Ortiz, I., *J. Chem. Technol. Biotechnol.*, 2017, vol. 92, no. 6, pp. 1167–1177. https://doi.org/10.1002/jctb.5186
24. Ayodele, B.V., Alsaffar, M.A., and Mustapa, S.I., *J. Cleaner Product.*, 2020, vol. 245, p. 118857. https://doi.org/10.1016/j.jclepro.2019.118857
25. Tokgoz, S., *Biofuels, Bioenergy and Food Security*, Elsevier, 2019, pp. 79–99. https://doi.org/10.1016/B978-0-12-803954-0.00005-X
26. Mueller, S.A., Anderson, J.E., and Wallington, T.J., *Biomass Bioenerg.*, 2011, vol. 35, no. 5, pp. 1623–1632. https://doi.org/10.1016/j.biombioe.2011.01.030
27. Katada, N., Iseki, Y., Shichi, A., Fujita, N., Ishino, I., Osaki, K., Torikai, T., and Niwa, M., *Appl. Catal. A: General*, 2008, vol. 349, nos. 1–2, pp. 55–61. https://doi.org/10.1016/j.apcata.2008.07.005
28. Hoseini, S.S., Najafi, G., Ghobadian, B., Mamat, R., Ebadi, M.T., and Yusaf, T., *Fuel*, 2018, vol. 220, pp. 621–630. https://doi.org/10.1016/j.fuel.2018.01.094
29. Vasil, R.G., *Strategic Research Program 2021*, Moscow: Technological Platform "BIOENERGETICS", 2021, vol. 6.
30. *Standard Specification for Biodiesel Fuel Blend Stock (B100) for Middle Distillate Fuels: ASTM D6751-20a*, 2023.
31. Hoekman, S.K., Broch, A., Robbins, C., Ceniceros, E., and Natarajan, M., *Renewab. Sustain. Energy Rev.*, 2012, vol. 16, no. 1, pp. 143–169. https://doi.org/10.1016/j.rser.2011.07.143
32. Haryanto, A., Hidayat, W., Hasanudin, U., Iryani, D.A., Kim, S., Lee, S., and Yoo, J., *Energies*, 2021, vol. 14, no. 5, p. 1407. https://doi.org/10.3390/en14051407
33. Datta, A., Hossain, A., and Roy, S., *Asian J. Chem.*, 2019, vol. 31, no. 8, pp. 1851–1858. https://doi.org/10.14233/ajchem.2019.22098
34. Madhu, P., Kanagasabapathy, H., and Neethi Manickam, I., *J. Material Cycles Waste Manag.*, 2016, vol. 18, no. 1, pp. 146–155. https://doi.org/10.1007/s10163-014-0318-y
35. Ighalo, J.O., Iwuchukwu, F.U., Eyankware, O.E., Iwuozor, K.O., Olotu, K., Bright, O.C., and Igwegbe, C.A., *Clean Technol. Environ. Policy*, 2022, vol. 24, no. 8, pp. 2349–2363. https://doi.org/10.1007/s10098-022-02339-5
36. Zhang, Q., Chang, J., Wang, T., and Xu, Y., *Energy Convers. Manag.*, 2007, vol. 48, no. 1, pp. 87–92. https://doi.org/10.1016/j.enconman.2006.05.010
37. Pourzolfaghar, H., Abnisa, F., Wan Daud, W.M.A., and Aroua, M.K., *J. Anal. Appl. Pyrol.*, 2018, vol. 133, pp. 117–127. https://doi.org/10.1016/j.jaap.2018.04.013
38. Li, Y., Zhang, C., Liu, Y., Tang, S., Chen, G., Zhang, R., and Tang, X., *Fuel*, 2017, vol. 189, pp. 23–31. https://doi.org/10.1016/j.fuel.2016.10.047
39. Aburto, J. and Amezcua-Allieri, M.A., *Biodiesel and Green Diesel Fuels: A Techno-Economic Analysis*, in *Green Diesel: An Alternative to Biodiesel and Petrodiesel. Advances in Sustainability Science and Technology*, Aslam, M., Shivaji Maktedar, S., and Sarma, A.K., Eds., Springer, Singapore, 2022, pp. 309–324. https://doi.org/10.1007/978-981-19-2235-0_11
40. Mortensen, P.M., Grunwaldt, J.-D., Jensen, P.A., Knudsen, K.G., and Jensen, A.D., *Appl. Catal. A: General*, 2011, vol. 407, nos. 1–2, pp. 1–19. https://doi.org/10.1016/j.apcata.2011.08.046
41. *U.S. Energy Information Administration, Gasoline and Diesel Fuel Update*, 2023. https://www.eia.gov/petroleum/gasdiesel/
42. Rytter, E., Hillestad, M., Austbø, B., Lamb, J.J., and Sarker, S., *Thermochemical Production of Fuels, Hydrogen, Biomass Bioenerg*, Elsevier, 2020, pp. 89–117. https://doi.org/10.1016/B978-0-08-102629-8.00006-2
43. Yi-Feng, C. and Wu, Q., *Biofuels*, Elsevier, 2011, pp. 399–413. https://doi.org/10.1016/B978-0-12-385099-7.00018-8
44. Daneshvar, E., Santhosh, C., Antikainen, E., and Bhatnagar, A., *J. Environ. Chem. Eng.*, 2018, vol. 6, no. 2, pp. 1848–1854. https://doi.org/10.1016/j.jece.2018.02.033
45. Isahak, W.N.R.W., Hisham, M.W.M., Yarmo, M.A., and Yun Hin, T., *Renewab. Sustain. Energy Rev.*, 2012, vol. 16, no. 8, pp. 5910–5923. https://doi.org/10.1016/j.rser.2012.05.039
46. Saber, M., Nakhshiniev, B., and Yoshikawa, K., *Renewab. Sustain. Energy Rev.*, 2016, vol. 58, pp. 918–930. https://doi.org/10.1016/j.rser.2015.12.342
47. Brennan, L. and Owende, P., *Renewab. Sustain. Energy Rev.*, 2010, vol. 14, no. 2, pp. 557–577. https://doi.org/10.1016/j.rser.2009.10.009
48. Fallah Kelarijani, A., Gholipour Zanjani, N., and Kamran Pirzaman, A., *Waste Biomass Valorizat.*, 2020, vol. 11, no. 6, pp. 2613–2621. https://doi.org/10.1007/s12649-019-00593-1
49. Karpagam, R., Jawaharraj, K., and Gnanam, R., *Sci. Total Environ.*, 2021, vol. 766, p. 144236. https://doi.org/10.1016/j.scitotenv.2020.144236
50. Meier, D., van de Beld, B., Bridgwater, A.V., Elliott, D.C., Oasmaa, A., and Preto, F., *Renewab. Sustain. Energy Rev.*, 2013, vol. 20, pp. 619–641. https://doi.org/10.1016/j.rser.2012.11.061

51. Yu, I.K.M., Chen, H., Abeln, F., Auta, H., Fan, J., Budarin, V.L., Clark, J.H., Parsons, S., Chuck, C.J., Zhang, S., Luo, G., and Tsang, D.C.W., *Critical Rev. Environ. Sci. Technol*., 2021, vol. 51, no. 14, pp. 1479–1532. https://doi.org/10.1080/10643389.2020.1753632
52. Kumar, B., Bhardwaj, N., Agrawal, K., Chaturvedi, V., and Verma, P., *Fuel Proc. Technol*., 2020, vol. 199, pp. 106244. https://doi.org/10.1016/j.fuproc.2019.106244
53. Yang, Z., Wu, Y., Zhang, Z., Li, H., Li, X., Egorov, R.I., Strizhak, P.A., and Gao, X., *Renewab. Sustain. Energy Rev*., 2019, vol. 103, pp. 384–398. https://doi.org/10.1016/j.rser.2018.12.047
54. Leibbrandt, N.H., Knoetze, J.H., and Görgens, J.F., *Biomass Bioenerg*., 2011, vol. 35, no. 5, pp. 2117–2126. https://doi.org/10.1016/j.biombioe.2011.02.017
55. Kumar, A., Jones, D., and Hanna, M., *Energies*, 2009, vol. 2, no. 3, pp. 556–581. https://doi.org/10.3390/en20300556
56. Nhuchehen, D.R., Basu, P., and Archarya, B., *Int. J. Renew. Energy Biofuel*., 2014, vol. 2014, p. 56. https://doi.org/10.5171/2014.506376
57. Osman, A.I., Mehta, N., Elgarahy, A.M., Al-Hinai, A., Al-Muhtaseb, A.H., and Rooney, D.W., *Environ. Chem. Lett*., 2021, vol. 19, no. 6, pp. 4075–4118. https://doi.org/10.1007/s10311-021-01273-0
58. Scarsella, M., de Caprariis, B., Damizia, M., and De Filippis, P., *Biomass Bioenerg*., 2020, vol. 140, pp. 105662. https://doi.org/10.1016/j.biombioe.2020.105662
59. Bridgwater, A.V., *Catal. Today*, 1996, vol. 29, nos. 1–4, pp. 285–295. https://doi.org/10.1016/0920-5861(95)00294-4
60. Kan, T., Strezov, V., and Evans, T.J., *Renewab. Sustain. Energy Rev*., 2016, vol. 57, pp. 1126–1140. https://doi.org/10.1016/j.rser.2015.12.185
61. Wang, M., Zhang, S.-L., and Duan, P.-G., *Energy Sources, Part A*, 2023, vol. 45, no. 1, pp. 2637–2650. https://doi.org/10.1080/15567036.2019.1665150
62. Amutio, M., Lopez, G., Artetxe, M., Elordi, G., Olazar, M., and Bilbao, J., *Res. Conserv. Recycl*., 2012, vol. 59, pp. 23–31. https://doi.org/10.1016/j.resconrec.2011.04.002
63. Himmel, M., Tucker, M., Baker, J., Rivard, C., Oh, K., and Grohmann, K., *Biotechnol. Bioenerg. Symp*., 1986.
64. Burhenne, L., Messmer, J., Aicher, T., and Laborie, M.-P., *J. Anal. Appl. Pyrol*., 2013, vol. 101, pp. 177–184. https://doi.org/10.1016/j.jaap.2013.01.012
65. Stals, M., Thijssen, E., Vangronsveld, J., Carleer, R., Schreurs, S., and Yperman, J., *J. Anal. Appl. Pyrol*., 2010, vol. 87, no. 1, pp. 1–7. https://doi.org/10.1016/j.jaap.2009.09.003
66. Alvarez, J., Lopez, G., Amutio, M., Bilbao, J., and Olazar, M., *Fuel*, 2014, vol. 128, pp. 162–169. https://doi.org/10.1016/j.fuel.2014.02.074
67. Venderbosch, R.H. and Prins, W., *Biofuel. Bioprod. Biorefinin*., 2010, vol. 4, no. 2, pp. 178–208. https://doi.org/10.1002/bbb.205
68. Blanquet, E. and Williams, P.T., *J. Anal. Appl. Pyrol*., 2021, vol. 159, pp. 105325. https://doi.org/10.1016/j.jaap.2021.105325
69. Rony, A.H., Kong, L., Lu, W., Dejam, M., Adidharma, H., Gasem, K.A.M., Zheng, Y., Norton, U., and Fan, M., *Biores. Technol*., 2019, vol. 284, pp. 466–473. https://doi.org/10.1016/j.biortech.2019.03.049
70. Wang, L., Ok, Y.S., Tsang, D.C.W., Alessi, D.S., Rinklebe, J., Wang, H., Mašek, O., Hou, R., O'Connor, D., and Hou, D., *Soil Use Manag*., 2020, vol. 36, no. 3, pp. 358–386. https://doi.org/10.1111/sum.12592
71. Heo, H.S., Park, H.J., Park, Y.-K., Ryu, C., Suh, D.J., Suh, Y.-W., Yim, J.-H., and Kim, S.-S., *Biores. Technol*., 2010, vol. 101, no. 1, pp. S91–S96. https://doi.org/10.1016/j.biortech.2009.06.003
72. Thangalazhy-Gopakumar, S., Adhikari, S., Ravindran, H., Gupta, R.B., Fasina, O., Tu, M., and Fernando, S.D., *Biores. Technol*., 2010, vol. 101, no. 21, pp. 8389–8395. https://doi.org/10.1016/j.biortech.2010.05.040
73. Ortega, J.V., Renehan, A.M., Liberatore, M.W., and Herring, A.M., *J. Anal. Appl. Pyrol*., 2011, vol. 91, no. 1, pp. 190–198. https://doi.org/10.1016/j.jaap.2011.02.007
74. Cao, J.-P., Xiao, X.-B., Zhang, S.-Y., Zhao, X.-Y., Sato, K., Ogawa, Y., Wei, X.-Y., and Takarada, T., *Biores. Technol*., 2011, vol. 102, no. 2, pp. 2009–2015. https://doi.org/10.1016/j.biortech.2010.09.057
75. Önal, E.P., Uzun, B.B., and Pütün, A.E., *Fuel Proc. Technol*., 2011, vol. 92, no. 5, pp. 879–885. https://doi.org/10.1016/j.fuproc.2010.12.006
76. Mullen, C.A., Boateng, A.A., Goldberg, N.M., Lima, I.M., Laird, D.A., and Hicks, K.B., *Biomass Bioenerg*., 2010, vol. 34, no. 1, pp. 67–74. https://doi.org/10.1016/j.biombioe.2009.09.012
77. Manyà, J.J., *Advanced Carbon Materials from Biomass: An Overview*, 2019. https://doi.org/10.5281/zenodo.3233733
78. Chen, X., Che, Q., Li, S., Liu, Z., Yang, H., Chen, Y., Wang, X., Shao, J., and Chen, H., *Fuel Proc. Technol*., 2019, vol. 196, p. 106180. https://doi.org/10.1016/j.fuproc.2019.106180
79. Balat, M., *Energ. Sourc., Part A*, 2008, vol. 30, no. 7, pp. 620–635. https://doi.org/10.1080/15567030600817258
80. Zhu, C., Maduskar, S., Paulsen, A.D., and Dauenhauer, P.J., *ChemCatChem*., 2016, vol. 8, no. 4, pp. 818–829.

https://doi.org/10.1002/cctc.201501235
81. Nzihou, A., Stanmore, B., Lyczko, N., and Minh, D.P., *Energy*, 2019, vol. 170, pp. 326–337. https://doi.org/10.1016/j.energy.2018.12.174
82. Nekhaev, A.I. and Maksimov, A.L., *Petrol. Chem.*, 2021, vol. 61, no. 1, pp. 15–34. https://doi.org/10.1134/S0965544121010023
83. Kibet, J., Khachatryan, L., and Dellinger, B., *Environ. Sci. Technol.*, 2012, vol. 46, no. 23, pp. 12994–13001. https://doi.org/10.1021/es302942c
84. Graça, I., Lopes, J.M., Ribeiro, M.F., Ramôa Ribeiro, F., Cerqueira, H.S., de Almeida, M.B.B., *Appl. Catal. B: Environmental*, 2011, vol. 101, nos. 3–4, pp. 613–621. https://doi.org/10.1016/j.apcatb.2010.11.002
85. Domine, M.E., van Veen, A.C., Schuurman, Y., and Mirodatos, C., *ChemSusChem.*, 2008, vol. 1, no. 3, pp. 179–181. https://doi.org/10.1002/cssc.200700049
86. Elliott, D.C. and Hart, T.R., *Energy Fuel.*, 2009, vol. 23, no. 2, pp. 631–637. https://doi.org/10.1021/ef8007773
87. Luque, R., Clark, J.H., Yoshida, K., and Gai, P.L., *Chem. Commun.*, 2009, no. 35, p. 5305. https://doi.org/10.1039/B911877B
88. Han, Y., Gholizadeh, M., Tran, C.-C., Kaliaguine, S., Li, C.-Z., Olarte, M., and Garcia-Perez, M.H, *Fuel Proc. Technol.*, 2019, vol. 195, p. 106140. https://doi.org/10.1016/j.fuproc.2019.106140
89. French, R.J., Hrdlicka, J., and Baldwin, R., *Environ. Progr. Sustain. Energy*, 2010, vol. 29, no. 2, pp. 142–150. https://doi.org/10.1002/ep.10419
90. Samolada, M.C., Baldauf, W., and Vasalos, I.A., *Fuel*, 1998, vol. 77, no. 14, pp. 1667–1675. https://doi.org/10.1016/S0016-2361(98)00073-8
91. Kim, P., Johnson, A., Edmunds, C.W., Radosevich, M., Vogt, F., Rials, T.G., and Labbé, N., *Energy Fuel.*, 2011, vol. 25, no. 10, pp. 4693–4703. https://doi.org/10.1021/ef200915s
92. Mortensen, P.M., Gardini, D., Damsgaard, C.D., Grunwaldt, J.-D., Jensen, P.A., Wagner, J.B., and Jensen, A.D., *Appl. Catal. A: General*, 2016, vol. 523, pp. 159–170. https://doi.org/10.1016/j.apcata.2016.06.002
93. Li, K., Wang, R., and Chen, J., *Energy Fuel.*, 2011, vol. 25, no. 3, pp. 854–863. https://doi.org/10.1021/ef101258j
94. Mortensen, P.M., Grunwaldt, J.-D., Jensen, P.A., and Jensen, A.D., *Catal. Today*, 2016, vol. 259, pp. 277–284. https://doi.org/10.1016/j.cattod.2015.08.022
95. de Caprariis, B., De Filippis, P., Petrullo, A., and Scarsella, M., *Fuel*, 2017, vol. 208, pp. 618–625. https://doi.org/10.1016/j.fuel.2017.07.054
96. Isahak, W.N.R.W., Hisham, M.W.M., Yarmo, M.A., and Yun Hin, T., *Renewab. Sustain. Energy Rev.*, 2012, vol. 16, no. 8, pp. 5910–5923. https://doi.org/10.1016/j.rser.2012.05.039
97. Lyu, G., Wu, S., Zhang, H., *Front, Energy Res.*, 2015, vol. 3. https://doi.org/10.3389/fenrg.2015.00028
98. Ambursa, M.M., Sudarsanam, P., Voon, L.H., Hamid, S.B.A., and Bhargava, S.K., *Fuel Proc. Technol.*, 2017, vol. 162, pp. 87–97. https://doi.org/10.1016/j.fuproc.2017.03.008
99. Doyle, A.M., Shaikhutdinov, S.K., Jackson, S.D., and Freund, H., *Ang. Chem. Int. Ed.*, 2003, vol. 42, no. 42, pp. 5240–5243. https://doi.org/10.1002/anie.200352124
100. Li, X., Chen, G., Liu, C., Ma, W., Yan, B., and Zhang, J., *Renewab. Sustain. Energy Rev.*, 2017, vol. 71, pp. 296–308. https://doi.org/10.1016/j.rser.2016.12.057
101. Zhang, X., Wang, T., Ma, L., Zhang, Q., Yu, Y., and Liu, Q., *Catal. Commun.*, 2013, vol. 33, pp. 15–19. https://doi.org/10.1016/j.catcom.2012.12.011
102. Tran, N.T.T., Uemura, Y., and Ramli, A., *Proc. Eng.*, 2016, vol. 148, pp. 1252–1258. https://doi.org/10.1016/j.proeng.2016.06.488
103. Vutolkina, A.V., Baigildin, I.G., Glotov, A.P., Pimerzin, Al.A., Akopyan, A.V., Maximov, A.L., and Karakhanov, E.A., *Appl. Catal. B: Environmental*, 2022, vol. 312, p. 121403. https://doi.org/10.1016/j.apcatb.2022.121403
104. Furimsky, E., *Appl. Catal. A: General*, 2000, vol. 199, no. 2, pp. 147–190. https://doi.org/10.1016/S0926-860X(99)00555-4
105. Gevert, B.S., Otterstedt, J.-E., and Massoth, F.E., *Appl. Catal.*., 1987, vol. 31, no. 1, pp. 119–131. https://doi.org/10.1016/S0166-9834(00)80671-5
106. Yakovlev, V.A., Bykova, M.V., and Khromova, S.A., *Catal. Industr.*, 2012, vol. 4, no. 4, pp. 324–339. https://doi.org/10.1134/S2070050412040204
107. Furimsky, E., *Catal. Rev.*, 1983, vol. 25, no. 3, pp. 421–458. https://doi.org/10.1080/01614948308078052
108. Viljava, T.-R., Komulainen, S., Selvam, T., and Krause, A.O., *Stud. Surf. Sci. Catal.*, 1999, vol. 127, pp. 145–152. https://doi.org/10.1016/S0167-2991(99)80403-0
109. Vogelzang, M., Li, C.-L., Schuit, G.C.A., Gates, B.C., and Petrakis, L., *J. Catal.*, 1983, vol. 84, no. 1, pp. 170–177. https://doi.org/10.1016/0021-9517(83)90095-7
110. Ambursa, M.M., Juan, J.C., Yahaya, Y., Taufiq-Yap, Y.H., Lin, Y.-C., and Lee, H.V., *Renewab. Sustain.*

Energy Rev., 2021, vol. 138, pp. 110667. https://doi.org/10.1016/j.rser.2020.110667
111. Ren, J., Cao, J.-P., and Zhao, X.-Y., *Appl. Energ. Combust. Sci*., 2022, vol. 9, pp. 100053. https://doi.org/10.1016/j.jaecs.2021.100053
112. Zhu, C., Cao, J.-P., Zhao, X.-Y., Xie, T., Zhao, M., and Wei, X.-Y., *Fuel Proc. Technol*., 2019, vol. 194, pp. 106126. https://doi.org/10.1016/j.fuproc.2019.106126
113. Tran, N.T.T., Uemura, Y., Chowdhury, S., and Ramli, A., *Appl. Catal. A: General*, 2016, vol. 512, pp. 93–100. https://doi.org/10.1016/j.apcata.2015.12.021
114. Mortensen, P.M., Grunwaldt, J.-D., Jensen, P.A., and Jensen, A.D., *ACS Catal*., 2013, vol. 3, no. 8, pp. 1774–1785. https://doi.org/10.1021/cs400266e
115. Li, G., Han, J., Wang, H., Zhu, X., and Ge, Q., *ACS Catal*., 2015, vol. 5, no. 3, pp. 2009–2016. https://doi.org/10.1021/cs501805y
116. Tan, Q., Wang, G., Nie, L., Dinse, A., Buda, C., Shabaker, J., and Resasco, D.E., *ACS Catal*., 2015, vol. 5, no. 11, pp. 6271–6283. https://doi.org/10.1021/acscatal.5b00765
117. Foraita, S., Fulton, J.L., Chase, Z.A., Vjunov, A., Xu, P., Baráth, E., Camaioni, D.M., Zhao, C., and Lercher, J.A., *Chemistry – A Eur. J*., 2015, vol. 21, no. 6, pp. 2423–2434. https://doi.org/10.1002/chem.201405312
118. Pan, Z., Wang, R., Nie, Z., and Chen, J., *J. Energ. Chem*., 2016, vol. 25, no. 3, pp. 418–426. https://doi.org/10.1016/j.jechem.2016.02.007
119. Bykova, M.V., Ermakov, D.Yu., Kaichev, V.V., Bulavchenko, O.A., Saraev, A.A., Lebedev, M.Yu., and Yakovlev, V.A., *Appl. Catal. B: Environmental*, 2012, vols. 113–114, pp. 296–307. https://doi.org/10.1016/j.apcatb.2011.11.051
120. Yao, Y. and Goodman, D.W., *J. Mol. Catal. A: Chemical*, 2014, vols. 383–384, pp. 239–242. https://doi.org/10.1016/j.molcata.2013.12.013
121. Khromova, S.A., Smirnov, A.A., Bulavchenko, O.A., Saraev, A.A., Kaichev, V.V., Reshetnikov, S.I., Yakovlev, V.A., *Appl. Catal. A: General*, 2014, vol. 470, pp. 261–270. https://doi.org/10.1016/j.apcata.2013.10.046
122. Guo, Q., Wu, M., Wang, K., Zhang, L., and Xu, X., *Industr. Eng. Chem. Res*., 2015, vol. 54, no. 3, pp. 890–899. https://doi.org/10.1021/ie5042935
123. Smirnov, A.A., Khromova, S.A., Ermakov, D.Yu., Bulavchenko, O.A., Saraev, A.A., Aleksandrov, P.V., Kaichev, V.V., and Yakovlev, V.A., *Appl. Catal. A: General*, 2016, vol. 514, pp. 224–234. https://doi.org/10.1016/j.apcata.2016.01.025
124. Smirnov, A.A., Geng, Zh., Khromova, S.A., Zavarukhin, S.G., Bulavchenko, O.A., Saraev, A.A., Kaichev, V.V., Ermakov, D.Yu., and Yakovlev, V.A., *J. Catal.*, 2017, vol. 354, pp. 61–77. https://doi.org/10.1016/j.jcat.2017.07.009
125. Vajglová, Z., Yevdokimova, O., Medina, A., Eränen, K., Tirri, T., Hemming, J., Lindén, J., Angervo, I., Damlin, P., Doronkin, D.E., Mäki-Arvela, P., and Murzin, D.Yu., *Sustain. Energy Fuel.*, 2023, vol. 7, no. 18, pp. 4486–4504. https://doi.org/10.1039/D3SE00371J
126. He, T., Liu, X., Ge, Y., Han, D., Li, J., Wang, Z., and Wu, J., *Catal. Commun*., 2017, vol. 102, pp. 127–130. https://doi.org/10.1016/j.catcom.2017.09.011
127. Li, K., Wang, R., and Chen, J., *Energy Fuel.*, 2011, vol. 25, no. 3, pp. 854–863. https://doi.org/10.1021/ef101258j
128. Argyle, M. and Bartholomew, C., *Catal*., 2015, vol. 5, no. 1, pp. 145–269. https://doi.org/10.3390/catal5010145
129. Zhao, C., Yu, Y., Jentys, A., and Lercher, J.A., *Appl. Catal. B: Environmental*, 2013, vols. 132–133, pp. 282–292. https://doi.org/10.1016/j.apcatb.2012.11.042
130. Dickinson, J.G. and Savage, P.E., *ACS Catal*., 2014, vol. 4, no. 8, pp. 2605–2615. https://doi.org/10.1021/cs500562u
131. Lee, C.R., Yoon, J.S., Suh, Y.-W., Choi, J.-W., Ha, J.-M., Suh, D.J., and Park, Y.-K., *Catal. Commun*., 2012, vol. 17, pp. 54–58. https://doi.org/10.1016/j.catcom.2011.10.011
132. Bie, Y., Lehtonen, J., and Kanervo, J., *Appl. Catal. A: General*, 2016, vol. 526, pp. 183–190. https://doi.org/10.1016/j.apcata.2016.08.030
133. Kulikov, L.A., Makeeva, D.A., Kalinina, M.A., Cherednichenko, K.A., Maximov, A.L., and Karakhanov, E.A., *Petrol. Chem.*, 2021, vol. 61, no. 7, pp. 711–720. https://doi.org/10.1134/S0965544121070045
134. Ruddy, D.A., Schaidle, J.A., Ferrell, III.J.R., Wang, J., Moens, L., and Hensley, J.E., *Green Chem*., 2014, vol. 16, no. 2, pp. 454–490. https://doi.org/10.1039/C3GC41354C
135. Besson, M., Descorme, C., Bernardi, M., Gallezot, P., di Gregorio, F., Grosjean, N., Pham Minh, D., and Pintar, A., *Environ. Technol.*, 2010, vol. 31, no. 13, pp. 1441–1447. https://doi.org/10.1080/09593331003628065
136. Wildschut, J., Mahfud, F.H., Venderbosch, R.H., and Heeres, H.J., *Industr. Eng. Chem. Res*., 2009, vol. 48, no. 23, pp. 10324–10334. https://doi.org/10.1021/ie9006003
137. Gutierrez, A., Kaila, R.K., Honkela, M.L., Slioor, R., and Krause, A.O.I., *Catal. Today*, 2009,

vol. 147, nod. 3–4, pp. 239–246.
https://doi.org/10.1016/j.cattod.2008.10.037
138. Zanuttini, M.S., Lago, C.D., Querini, C.A., and Peralta, M.A., *Catal. Today*, 2013, vol. 213, pp. 9–17.
https://doi.org/10.1016/j.cattod.2013.04.011
139. Karakhanov, E.A., Boronoev, M.P., Filippova, T.Yu., and Maksimov, A.L., *Petrol. Chem.*, 2018, vol. 58, no. 5, pp. 407–411.
https://doi.org/10.1134/S0965544118050080
140. Foster, A.J., Do, P.T.M., and Lobo, R.F., *Topics in Catal.*, 2012, vol. 55, nos. 3–4, pp. 118–128.
https://doi.org/10.1007/s11244-012-9781-7
141. Hong, Y., Zhang, H., Sun, J., Ayman, K.M., Hensley, A.J.R., Gu, M., Engelhard, M.H., McEwen, J.-S., and Wang, Y., *ACS Catal.*, 2014, vol. 4, no. 10, pp. 3335–3345.
https://doi.org/10.1021/cs500578g
142. Hong, Y.-K., Lee, D.-W., Eom, H.-J., and Lee, K.-Y., *Appl. Catal. B: Environmental*, 2014, vols. 150–151, pp. 438–445.
https://doi.org/10.1016/j.apcatb.2013.12.045
143. Echeandia, S., Pawelec, B., Barrio, V.L., Arias, P.L., Cambra, J.F., Loricera, C.V., and Fierro, J.L.G., *Fuel*, 2014, vol. 117, pp. 1061–1073.
https://doi.org/10.1016/j.fuel.2013.10.011
144. Karakhanov, E., Maximov, A., Terenina, M., Vinokurov, V., Kulikov, L., Makeeva, D., and Glotov, A., *Catal. Today*, 2020, vol. 357, pp. 176–184.
https://doi.org/10.1016/j.cattod.2019.05.028
145. Hensley, A.J.R., Wang, Y., and McEwen, J.-S., *Surface Sci.*, 2014, vol. 630, pp. 244–253.
https://doi.org/10.1016/j.susc.2014.08.003
146. Ardiyanti, A.R., Gutierrez, A., Honkela, M.L., Krause, A.O.I., and Heeres, H.J., *Appl. Catal. A: General*, 2011, vol. 407, nos. 1–2, pp. 56–66.
https://doi.org/10.1016/j.apcata.2011.08.024
147. Gao, D., Schweitzer, C., Hwang, H.T., and Varma, A., *Industr. Eng. Chem. Res.*, 2014, vol. 53, no. 49, pp. 18658–18667.
https://doi.org/10.1021/ie500495z
148. Roldugina, E.A., Naranov, E.R., Maximov, A.L., and Karakhanov, E.A., *Appl. Catal. A: General*, 2018, vol. 553, pp. 24–35.
https://doi.org/10.1016/j.apcata.2018.01.008
149. Shakirov, I.I., Boronoev, M.P., Zolotukhina, A.V., Maximov, A.L., and Karakhanov, E.A., *Petrol. Chem.*, 2020, vol. 60, no. 10, pp. 1136–1140.
https://doi.org/10.1134/S0965544120100102
150. Li, W., Wang, H., Wu, X., Betancourt, L.E., Tu, C., Liao, M., Cui, X., Li, F., Zheng, J., and Li, R., *Fuel*, 2020, vol. 274, p. 117859.
https://doi.org/10.1016/j.fuel.2020.117859
151. Dang, R., Ma, X., Luo, J., Zhang, Y., Fu, J., Li, C., and Yang, N., *J. Energ. Inst.*, 2020, vol. 93, no. 4, pp. 1527–1534.
https://doi.org/10.1016/j.joei.2020.01.015
152. Sankaranarayanan, T.M., Berenguer, A., Ochoa Hernández, C., Moreno, I., Jana, P., Coronado, J.M., Serrano, D.P., and Pizarro, P., *Catal. Today*, 2015, vol. 243, pp. 163–172.
https://doi.org/10.1016/j.cattod.2014.09.004
153. Roldugina, E.A., Shayakhmetov, N.N., Maksimov, A.L., and Karakhanov, E.A., *Russ. J. Appl. Chem.*, 2019, vol. 92, no. 9, pp. 1306–1315.
https://doi.org/10.1134/S1070427219090167
154. Bjelić, A., Grilc, M., Huš, M., and Likozar, B., *Chem. Eng. J.*, 2019, vol. 359, pp. 305–320.
https://doi.org/10.1016/j.cej.2018.11.107
155. Žula, M., Grilc, M., and Likozar, B., *Chem. Eng. J.*, 2022, vol. 444, p. 136564.
https://doi.org/10.1016/j.cej.2022.136564
156. Tieuli, S., Mäki-Arvela, P., Peurla, M., Eränen, K., Wärnå, J., Cruciani, G., Menegazzo, F., Murzin, D.Yu., and Signoretto, M., *Appl. Catal. A: General*, 2019, vol. 580, pp. 1–10.
https://doi.org/10.1016/j.apcata.2019.04.028
157. Liu, Q., Zuo, H., Zhang, Q., Wang, T., and Ma, L., *Chinese J. Catal.*, 2014, vol. 35, no. 5, pp. 748–756.
https://doi.org/10.1016/S1872-2067(12)60710-4
158. Weingarten, R., Tompsett, G.A., Conner, W.C., Huber, G.W., *J. Catal.*, 2011, vol. 279, no. 1, pp. 174–182.
https://doi.org/10.1016/j.jcat.2011.01.013
159. Zacharopoulou, V. and Lemonidou, A., *Catal.*, 2017, vol. 8, no. 1, p. 2.
https://doi.org/10.3390/catal8010002
160. Santacesaria, E., *J. Catal.*, 1984, vol. 90, no. 1, pp. 1–9.
https://doi.org/10.1016/0021-9517(84)90077-0
161. Weitkamp, J., *Solid State Ion.*, 2000, vol. 131, nos. 1–2, pp. 175–188.
https://doi.org/10.1016/S0167-2738(00)00632-9
162. Zhao, C., Kasakov, S., He, J., and Lercher, J.A., *J. Catal.*, 2012, vol. 296, pp. 12–23.
https://doi.org/10.1016/j.jcat.2012.08.017
163. Ohta, H., Yamamoto, K., Hayashi, M., Hamasaka, G., Uozumi, Y., and Watanabe, Y., *Chem. Commun.*, 2015, vol. 51, no. 95, pp. 17000–17003.
https://doi.org/10.1039/C5CC05607A
164. Song, W., Liu, Y., Baráth, E., Zhao, C., and Lercher, J.A., *Green Chem.*, 2015, vol. 17, no. 2, pp. 1204–1218.
https://doi.org/10.1039/C4GC01798F
165. Resasco, D.E., *J. Phys. Chem. Lett.*, 2011, vol. 2, no. 18, pp. 2294–2295.
https://doi.org/10.1021/jz201135x

166. Graça, I., Comparot, J.-D., Laforge, S., Magnoux, P., Lopes, J.M., Ribeiro, M.F., and Ramôa Ribeiro, F., *Energy Fuel.*, 2009, vol. 23, no. 9, pp. 4224–4230. https://doi.org/10.1021/ef9003472
167. Serrano, D.P., Melero, J.A., Coronado, J.M., Pizarro, P., and Morales, G., in *Zeolites in Catalysis: Properties and Applications*, Čejka, J., Morris, R.E., and Nachtigall, P., Eds., The Royal Society of Chemistry, 2017, ch. 12, pp. 441–480. https://doi.org/10.1039/9781788010610
168. Wang, C., Tian, Z., Wang, L., Xu, R., Liu, Q., Qu, W., Ma, H., and Wang, B., *ChemSusChem.*, 2012, vol. 5, no. 10, pp. 1974–1983. https://doi.org/10.1002/cssc.201200219
169. Shafaghat, H., Sirous Rezaei, P., and Daud, W.M.A.W., *RSC Adv.*, 2015, vol. 5, no. 43, pp. 33990–33998. https://doi.org/10.1039/C5RA00367A
170. Berenguer, A., Bennett, J.A., Hunns, J., Moreno, I., Coronado, J.M., Lee, A.F., Pizarro, P., Wilson, K., and Serrano, D.P., *Catal. Today*, 2018, vol. 304, pp. 72–79. https://doi.org/10.1016/j.cattod.2017.08.032
171. Lee, H.W., Jun, B.R., Kim, H., Kim, D.H., Jeon, J.-K., Park, S.H., Ko, C.H., Kim, T.-W., and Park, Y.-K., *Energy*, 2015, vol. 81, pp. 33–40. https://doi.org/10.1016/j.energy.2014.11.058
172. Peng, B., Yao, Y., Zhao, C., and Lercher, J.A., *Ang. Chemie Inter. Ed.*, 2012, vol. 51, no. 9, pp. 2072–2075. https://doi.org/10.1002/anie.201106243
173. Wang, L., Zhang, J., Yi, X., Zheng, A., Deng, F., Chen, C., Ji, Y., Liu, F., Meng, X., and Xiao, F.-S., *ACS Catal.*, 2015, vol. 5, no. 5, pp. 2727–2734. https://doi.org/10.1021/acscatal.5b00083
174. Lee, H., Kim, Y.-M., Jung, K.B., Jae, J., Jung, S.-C., Jeon, J.-K., and Park, Y.-K., *J. Clean. Product.*, 2018, vol. 174, pp. 763–770. https://doi.org/10.1016/j.jclepro.2017.10.315
175. Wang, Y., He, T., Liu, K., Wu, J., and Fang, Y., *Biores. Technol.*, 2012, vol. 108, pp. 280–284. https://doi.org/10.1016/j.biortech.2011.12.132
176. Tyrone Ghampson, I., Sepúlveda, C., Garcia, R., García Fierro, J.L., Escalona, N., and DeSisto, W.J., *Appl. Catal. A: General*, 2012, vols. 435–436, pp. 51–60. https://doi.org/10.1016/j.apcata.2012.05.039
177. Al Othman, Z., *Material.*, 2012, vol. 5, no. 12, pp. 2874–2902. https://doi.org/10.3390/ma5122874
178. Khalil, K.M.S., *J. Colloid Interface Sci.*, 2007, vol. 315, no. 2, pp. 562–568. https://doi.org/10.1016/j.jcis.2007.07.030
179. Yoon, J.S., Lee, T., Choi, J.-W., Suh, D.J., Lee, K., Ha, J.-M., and Choi, J., *Catal. Today*, 2017, vols. 293–294, pp. 142–150. https://doi.org/10.1016/j.cattod.2016.10.033
180. Newman, C., Zhou, X., Goundie, B., Ghampson, I.T., Pollock, R.A., Ross, Z., Wheeler, M.C., Meulenberg, R.W., Austin, R.N., and Frederick, B.G., *Appl. Catal. A: General*, 2014, vol. 477, pp. 64–74. https://doi.org/10.1016/j.apcata.2014.02.030
181. Ziolek, M., Nowak, I., and Lavalley, J.C., *Catal. Lett.*, 1997, vol. 45, nos. 3–4, pp. 259–265. https://doi.org/10.1023/A:1019000619962
182. Kosslick, H., Lischke, G., Parlitz, B., Storek, W., and Fricke, R., *Appl. Catal. A: General*, 1999, vol. 184, no. 1, pp. 49–60. https://doi.org/10.1016/S0926-860X(99)00078-2
183. Feng, L., Li, X., Wang, Z., and Liu, B., *Biores. Technol.*, 2021, vol. 323, p. 124569. https://doi.org/10.1016/j.biortech.2020.124569
184. Molina-Conde, L.H., Suárez-Méndez, A., Pérez Estrada, D.E., and Klimova, T.E., *Appl. Catal. A: General*, 2023, vol. 663, p. 119313. https://doi.org/10.1016/j.apcata.2023.119313
185. Taghvaei, H., Moaddeli, A., Khalafi-Nezhad, A., and Iulianelli, A., *Fuel*, 2021, vol. 293, p. 120493. https://doi.org/10.1016/j.fuel.2021.120493
186. Sirous-Rezaei, P., Jae, J., Ha, J.-M., Ko, C.H., Kim, J.M., Jeon, J.-K., and Park, Y.-K., *Green Chem.*, 2018, vol. 20, no. 7, pp. 1472–1483. https://doi.org/10.1039/C7GC03823B
187. Szczyglewska, P., Feliczak-Guzik, A., and Nowak, I., *Micropor. Mesopor. Mater.*, 2020, vol. 293, p. 109771. https://doi.org/10.1016/j.micromeso.2019.109771
188. Bejblová, M., Zámostný, P., Červený, L., and Čejka, J., *Appl. Catal. A: General*, 2005, vol. 296, no. 2, pp. 169–175. https://doi.org/10.1016/j.apcata.2005.07.061
189. Yang, X., Zhang, S., Qiu, Z., Tian, G., Feng, Y., and Xiao, F.-S., *J. Phys. Chem. B*, 2004, vol. 108, no. 15, pp. 4696–4700. https://doi.org/10.1021/jp0380226
190. Glotov, A., Vutolkina, A., Pimerzin, A., Nedolivko, V., Zasypalov, G., Stytsenko, V., Karakhanov, E., and Vinokurov, V., *Catal.*, 2020, vol. 10, no. 5, p. 537. https://doi.org/10.3390/catal10050537
191. Lvov, Y., Wang, W., Zhang, L., and Fakhrullin, R., *Adv. Mater.*, 2016, vol. 28, no. 6, pp. 1227–1250. https://doi.org/10.1002/adma.201502341
192. Glotov, A., Vutolkina, A., Pimerzin, A., Vinokurov, V., and Lvov, Y., *Chem. Soc. Rev.*, 2021, vol. 50, no. 16, pp. 9240–9277. https://doi.org/10.1039/D1CS00502B
193. Stavitskaya, A., Rubtsova, M., Glotov, A., Vinokurov, V., Vutolkina, A., Fakhrullin, R., and Lvov, Y., *Nanoscale*

Adv., 2022, vol. 4, no. 13, pp. 2823–2835. https://doi.org/10.1039/D2NA00163B
194. Vutolkina, A.V., Zasypalov, G.O., Aljajan, Ya., Klimovsky, V.A., Vinokurov, V.A., Rubtsova, M.I., Pimerzin, Al.A., and Glotov, A.P., *New J. Chem*., 2023, vol. 47, no. 25, pp. 12015–12026. https://doi.org/10.1039/D3NJ01709E
195. Demikhova, N.R., Rubtsova, M.I., Kireev, G.A., Cherednichenko, K.A., Vinokurov, V.A., and Glotov, A.P., *Chem. Eng. J*., 2023, vol. 453, pp. 139581. https://doi.org/10.1016/j.cej.2022.139581
196. Singh, B. and Mackinnon, I.D.R., *Clays Clay Miner.*, 1996, vol. 44, pp. 825–834. https://doi.org/10.1346/CCMN.1996.0440614
197. Glotov, A.P., Roldugina, E.A., Artemova, M.I., Smirnova, E.M., Demikhova, N.R., Stytsenko, V.D., Egazar'yants, S.V., Maksimov, A.L., and Vinokurov, V.A., *Russ. J. Appl. Chem*., 2018, vol. 91, no. 8, pp. 1353–1362. https://doi.org/10.1134/S1070427218080141
198. Stehl, D., Milojević, N., Stock, S., Schomäcker, R., and von Klitzing, R., *Industr. Eng. Chem. Res*., 2019, vol. 58, no. 7, pp. 2524–2536. https://doi.org/10.1021/acs.iecr.8b04619
199. Stavitskaya, A., Mazurova, K., Kotelev, M., Eliseev, O., Gushchin, P., Glotov, A., Kazantsev, R., Vinokurov, V., and Lvov, Y., *Molecules*, 2020, vol. 25, no. 8, p. 1764. https://doi.org/10.3390/molecules25081764
200. Akopyan, A., Polikarpova, P., Vutolkina, A., Cherednichenko, K., Stytsenko, V., and Glotov, A., *Pure Appl. Chem*., 2021, vol. 93, no. 2, pp. 231–241. https://doi.org/10.1515/pac-2020-0901
201. Glotov, A.P., Vutolkina, A.V., Vinogradov, N.A., Pimerzin, A.A., Vinokurov, V.A., and Pimerzin, Al.A., *Catal. Today*, 2021, vol. 377, pp. 82–91. https://doi.org/10.1016/j.cattod.2020.10.010
202. Zasypalov, G., Vutolkina, A., Klimovsky, V., Abramov, E., Vinokurov, V., and Glotov, A., *Appl. Catal. B: Environmental*, 2023, vol. 342, p. 123425. https://doi.org/10.1016/j.apcatb.2023.123425
203. Serrano-Maldonado, A., Bendounan, A., Silly, M.G., Pla, D., and Gómez, M., *ACS Appl. Nano Mater*., 2023, vol. 6, no. 13, pp. 11317–11326. https://doi.org/10.1021/acsanm.3c01361
204. Zhang, Z., Song, J., and Han, B., *Chem. Rev*., 2017, vol. 117, no. 10, pp. 6834–6880. https://doi.org/10.1021/acs.chemrev.6b00457
205. Vinokurov, V., Glotov, A., Chudakov, Y., Stavitskaya, A., Ivanov, E., Gushchin, P., Zolotukhina, A., Maximov, A., Karakhanov, E., and Lvov, Y., *Industr. Eng. Chem. Res*., 2017, vol. 56, no. 47, pp. 14043–14052. https://doi.org/10.1021/acs.iecr.7b03282
206. Nedolivko, V.V., Zasypalov, G.O., Chudakov, Ya.A., Vutolkina, A.V., Pimerzin, Al.A., and Glotov, A.P., *Russ. Chem. Bull*., 2020, vol. 69, no. 2, pp. 260–264. https://doi.org/10.1007/s11172-020-2754-2
207. Nedolivko, V.V., Zasypalov, G.O., Boev, S.S., Cherednichenko, K.A., Vinokurov, V.A., and Glotov, A.P., *Petrol. Chem.*, 2021, vol. 61, no. 10, pp. 1104–1110. https://doi.org/10.1134/S0965544121100017
208. Vutolkina, A., Glotov, A., Baygildin, I., Akopyan, A., Talanova, M., Terenina, M., Maximov, A., and Karakhanov, E., *Pure Appl. Chem*., 2020, vol. 92, no. 6, pp. 949–966. https://doi.org/10.1515/pac-2019-1115
209. Glotov, A., Novikov, A., Stavitskaya, A., Nedolivko, V., Kopitsyn, D., Kuchierskaya, A., Ivanov, E., Stytsenko, V., Vinokurov, V.,and Lvov, Y., *Catal. Today*, 2021, vol. 378, pp. 33–42. https://doi.org/10.1016/j.cattod.2020.10.001
210. Fu, L., Yang, H., Tang, A., and Hu, Y., *Nano Res*., 2017, vol. 10, no. 8, pp. 2782–2799. https://doi.org/10.1007/s12274-017-1482-x
211. Mäki-Arvela, P. and Murzin, D., *Catal*., 2017, vol. 7, no. 9, pp. 265. https://doi.org/10.3390/catal7090265